Arabidopsis and Maize Terminator Strength is Determined by GC Content, Polyadenylation Motifs and Cleavage Probability

Sayeh Gorjifard[1], Tobias Jores[1], Jackson Tonnies[1,2], Nicholas A Mueth[1], Kerry Bubb[1], Travis Wrightsman[3], Edward S Buckler[3,4,5], Stanley Fields[1,6], Josh T Cuperus[1], Christine Queitsch[1,7]

[1] Department of Genome Sciences, University of Washington, Seattle, WA 98195.
[2] Graduate Program in Biology, University of Washington, Seattle, WA 98195.
[3] Section of Plant Breeding and Genetics, Cornell University, Ithaca, NY 14853.
[4] Agricultural Research Service, United States Department of Agriculture, Ithaca, NY 14853.
[5] Institute for Genomic Diversity, Cornell University, Ithaca, NY 14853.
[6] Department of Medicine, University of Washington, Seattle, WA 98195.
[7] Corresponding Author: Christine Queitsch, queitsch@uw.edu

Abstract

The 3' end of a gene, often called a terminator, modulates mRNA stability, localization, translation, and polyadenylation. Here, we adapted Plant STARR-seq, a massively parallel reporter assay, to measure the activity of over 50,000 terminators from the plants *Arabidopsis thaliana* and *Zea mays*. We characterize thousands of plant terminators, including many that outperform bacterial terminators commonly used in plants. Terminator activity is species-specific, differing in tobacco leaf and maize protoplast assays. While recapitulating known biology, our results reveal the relative contributions of polyadenylation motifs to terminator strength. We built a computational model to predict terminator strength and used it to conduct *in silico* evolution that generated optimized synthetic terminators. Additionally, we discover alternative polyadenylation sites across tens of thousands of terminators; however, the strongest terminators tend to have a dominant cleavage site. Our results establish features of plant terminator function and identify strong naturally occurring and synthetic terminators.

Introduction

A critical challenge is producing enough food for a growing world population that is likely to reach over 9 billion people by the year 2050 (Department of Economic and Social Affairs 2022). Food security can be bolstered through crop engineering, which can improve yields and increase tolerance to pathogens and environmental stresses (Hickey et al. 2019; Eshed and Lippman 2019). However, for crop engineering to be successful, precise control over transgene expression is required. In plants, past efforts to optimize critical *cis*-elements have mostly focused on the identification, characterization, and manipulation of upstream regulatory elements such as promoters (Jores et al. 2021, 2020; Zhou et al. 2023; X. Wang et al. 2021; Rodríguez-Leal et al. 2017). Although these upstream elements can produce large effects on gene expression, other sequence elements also contribute. For example, the 3' end of a gene contains sequence motifs necessary for mRNA 3' end maturation, cleavage, and polyadenylation (Kumar et al. 2019; A. G. Hunt 1994; Arthur G. Hunt 2011; Felipe F. de Felippes and Waterhouse 2023; Loke et al. 2005; B. Tian and Graber 2012; Rothnie, Reid, and Hohn 1994; Rothnie 1996). In keeping with established nomenclature (Brooks et al. 2023; Felipe F. de Felippes and Waterhouse 2023; C. Tian et al. 2022), throughout this manuscript, we refer to sequences surrounding a cleavage and polyadenylation site as terminators.

Terminators also affect mRNA stability, nuclear export, and translation (Felipe F. de Felippes and Waterhouse 2023). Moreover, terminators play a central role in transgene silencing mediated by small RNAs (Baeg, Iwakawa, and Tomari 2017; Allen and Howell 2010; Qin et al. 2012; Diamos and Mason 2018; F de Felippes et al. 2020).

Messenger RNA cleavage and polyadenylation are tightly linked to and initiate transcription termination (Connelly and Manley 1988; Birse et al. 1998; Proudfoot 2011; Whitelaw and Proudfoot 1986); however, termination occurs up to 1 kb downstream of the mRNA cleavage site (Mo et al. 2021). The current model of how mRNA 3' end processing leads to transcription termination combines features of two previously proposed models (Rosonina, Kaneko, and Manley 2006; Luo, Johnson, and Bentley 2006; Eaton and West 2020; Krzyszton et al. 2018): After mRNA cleavage, conformational changes of RNA polymerase II allosterically reduce its elongation rate (allosteric model). At the same time, the cleavage site enables a 5′ to 3' exonuclease (Rat1 in yeast, XRN2 in humans, and XRN3 in *Arabidopsis*) to degrade the downstream RNA and initiate transcription termination when it catches up with the RNA polymerase (torpedo model). The exact site of transcription termination can further be affected by RNA polymerase II pause sites, R loops formed between DNA and the nascent RNA, and DNA-binding proteins (Eaton and West 2020; Yu, Martin, and Michaels 2019).

Although the choice of terminator significantly impacts transgene expression, only a few terminators — often those derived from viruses or bacteria — are commonly used in crop engineering. These viral or bacterial sequences make transgene silencing more likely (Dadami et al. 2014; Diamos and Mason 2018). Compared to the commonly used *Agrobacterium tumefaciens* nopaline synthase terminator (tNOS), the terminator from the *Arabidopsis thaliana* heat shock protein 18.2 results in increased transgene expression and mRNA stability, and decreased silencing (Nagaya et al. 2010; Hirai et al. 2011; Pérez-González and Caro 2018; F de Felippes et al. 2020; Felipe Fenselau de Felippes, Shand, and Waterhouse 2022). This finding highlights the need to characterize and optimize native plant terminators as building blocks for crop engineering applications (Ingelbrecht et al. 1989; Diamos and Mason 2018; C. Tian et al. 2022).

Plant terminators have been characterized by analysis of wild-type and mutated versions of a handful of terminators, from both plant and non-plant sources, or by searching for motifs enriched in genomic sequences surrounding mRNA cleavage sites. These studies established three main *cis*-acting elements required for 3' end processing (A. G. Hunt 1994; Shen et al. 2008; Loke et al. 2005; Bernardes and Menossi 2020; Felipe F. de Felippes and Waterhouse 2023). The first element is the far upstream element (FUE), which resides in a U-rich region located 30 – 150 nucleotides upstream of the cleavage site and often contains one or more UGUA sequences. The second is the near upstream element (NUE), which resides in an A-rich region located 10 – 30 nucleotides upstream of the cleavage site and contains the polyadenylation signal AAUAAA. The third is the cleavage element (CE), which contains the cleavage site, formed by a UA or CA dinucleotide embedded in a U-rich region. Although the general pattern and nucleotide preferences of *cis*-acting elements in plant terminators are known, their relative contributions to terminator strength and species specificity have not been determined.

Here, we characterized over 50,000 terminators from the model plant *Arabidopsis thaliana* and the crop plant maize (*Zea mays*). We identified sequence features contributing to terminator strength and quantified their effect on transcript levels. By measuring terminator strength in two assay systems—tobacco leaves and maize protoplasts—we detected similarities and differences in the terminator grammar of monocotyledonous and dicotyledonous plants. Leveraging our large dataset, we trained computational models that accurately predict terminator strength. We used these models to design robust synthetic plant terminators for future crop engineering efforts.

Results

Measuring the strength of plant terminators with Plant STARR-seq

To assess the strength of plant terminators at high throughput, we used Plant STARR-seq, a massively parallel reporter assay that measures the activity of cis-regulatory elements (Jores et al. 2020, 2021). The average 3' untranslated region (UTR) length in *Arabidopsis* and maize is 242 bp and 310 bp, respectively (Srivastava 2018; Jafar 2019). However, due to technical limitations in DNA array-synthesis, we were limited to sequences of 170 nucleotides. Previous studies on plant terminators revealed that most elements required for efficient mRNA 3' end processing reside within approximately 150 bp upstream of the cleavage and polyadenylation site (Loke et al. 2005; A. G. Hunt 1994; Shen et al. 2008; Bernardes and Menossi 2020; Felipe F. de Felippes and Waterhouse 2023; Rothnie 1996). Furthermore, studies in yeast and animals revealed that sequence elements downstream of the cleavage site can also affect polyadenylation (B. Tian and Graber 2012; Bernardes and Menossi 2020; Felipe F. de Felippes and Waterhouse 2023). Although such elements have not been reported in plants, we included the 20 nucleotides downstream of the cleavage site in our candidate sequences to test if they have an effect of terminator activity. For these reasons, we defined a terminator as the 170 nucleotide sequence from position -150 to +20 relative to a cleavage and polyadenylation site (position 0) in this study. We used experimentally derived primary cleavage sites to select terminator sequences from wild-type Arabidopsis and maize (Jafar et al. 2019; Thomas et al. 2012; Wu et al. 2011). For the 3,754 Arabidopsis genes that were not represented in these datasets, we used the end of the 3' untranslated region (UTR) annotation in TAIR10 as the cleavage site. Since alternative polyadenylation plays an important role in gene regulation by creating different mRNA isoforms (Arthur G. Hunt 2011), we sought to investigate the strength of both primary and secondary polyadenylation sites. Therefore, we included experimentally-derived, secondary cleavage sites supported by at least 30% of the total reads of a gene (Jafar et al. 2019; Thomas et al. 2012; Wu et al. 2011). As expected, the 24,529 Arabidopsis terminators and the 30,092 maize terminators displayed the distinctive nucleotide composition preferences of terminator sequences (Bernardes and Menossi 2020) and predominantly resided in the annotated 3' UTR region (Supplementary Fig. 1a-d).

The library of plant terminators was array-synthesized and cloned downstream of the coding sequence of a barcoded green fluorescent protein (GFP) reporter gene driven by the cauliflower mosaic virus 35S promoter (Fig. 1a). The plasmid library was transiently expressed in tobacco leaves or maize protoplasts. After 1 – 2 days of incubation, the reporter mRNA was extracted, and next-generation sequencing was used to count the reporter barcodes in the input DNA and the extracted RNA. Strong terminators yield higher transcript levels due to improved 3' end processing or transcript stability as compared to weak terminators (Felippes 2023; Bernardes 2020). The number of transcripts (i.e. RNA reads) per DNA template (i.e. DNA reads) is therefore a direct measure of the strength of a terminator. We define terminator strength as the enrichment of barcodes in RNA over DNA normalized to the enrichment of a control construct containing the 35S terminator. Thus, terminator strength in our assay reflects both transcriptional activity and RNA stability, and tends to have low values due to the normalization to the highly active 35S terminator.

We performed two biological replicates in tobacco leaves and maize protoplasts. The results were highly correlated in both assay systems (Fig. 1b, c). Similarly, retesting of over 400 terminators in a second, independent library showed that the replicates in this validation experiment were highly correlated with each other and with the results of the first, large-scale experiment (Supplementary Fig. 2). Therefore, we used the average terminator strength from both replicates of the large-scale experiment for all further analyses. Terminator strength spanned a wide range of activity, allowing us to disentangle the signals that contribute to this

145 strength. In tobacco leaves, we observed more than 64-fold difference between strong and
146 weak terminators. Similar to previous studies (Jores et al. 2021, 2020), the dynamic range was
147 lower in maize protoplasts, in which we detected a 16-fold difference between strong and weak
148 terminators.
149 To ensure that we measured terminator strength, we included negative controls derived
150 from coding regions in *Arabidopsis* and maize and from randomized sequences. The random
151 sequences were generated such that their overall (global random) or per-position (positional
152 random) nucleotide frequencies resembled that of an average *Arabidopsis* or maize terminator
153 (Supplementary Fig. 1e-g). In both tobacco leaves and maize protoplasts, sequences derived
154 from plant terminators outperformed these coding sequences and random controls (Fig. 1d, e).
155 Of all control sequences, the positional random sequences showed the greatest strength, likely
156 because they most closely resemble actual terminators. Together, these findings demonstrate
157 that our assay captures *bona fide* terminator strength.
158 We sought to confirm our measure of terminator strength by Plant STARR-seq with an
159 orthogonal assay. To do so, we conducted a dual-luciferase assay in both tobacco leaves and
160 maize protoplasts for several weak, intermediate, and strong terminators. We observed a strong
161 correlation between terminator strength measured by the two assays (Supplementary Fig. 3b,
162 d). Strong terminators yielded higher nanoluciferase activity than weak terminators
163 (Supplementary Fig. 3a, c).
164 Most plant transgenes use viral or bacterial terminators, such as the 35S, Ag7, NOS,
165 and MAS terminators (Andreou et al. 2021). We included these terminators in our library in their
166 full form (not limited to 170 nucleotides) as a reference for the activity of the plant terminators.
167 The 35S terminator, the only viral sequence in our library, outperformed almost all plant
168 terminators. However, some plant terminators (8 in tobacco leaves and 20 in maize protoplasts)
169 exceeded the activity of the 35S terminator. The bacterial Ag7, NOS, and MAS terminators were
170 far weaker than the viral 35S terminator. In tobacco leaves, we found 2,224 plant terminators
171 that were stronger than the MAS terminator and 9,389 plant terminators that were stronger than
172 the NOS terminator. In maize protoplasts, we found 1,369 plant terminators that were stronger
173 than the MAS terminator and 19,585 terminators that were stronger than the NOS terminator.
174 The strongest plant terminators are attractive alternatives to the bacterial terminators commonly
175 used in plant transgenes.

176 Terminator strength correlates not with gene expression but with gene function

177 Next, we asked if our data could give insights into the importance of terminator strength
178 for gene expression. We compared terminator strength determined by Plant STARR-seq with
179 metrics related to mRNA levels, stability and degradation. We found only weak correlation
180 between terminator strength and gene expression (Sullivan et al. 2014), mRNA half-life (Szabo
181 et al. 2020), or nascent transcription (Liu, Zhu, and Dong 2021) (Supplementary Fig. 4). These
182 findings corroborate reports that upstream *cis*-regulatory elements, like enhancers, promoters,
183 and the 5' UTR, drive large-scale gene expression changes while the 3' UTR and terminators
184 fine-tune expression levels (Washburn et al. 2019; Zrimec et al. 2020). However, the choice of
185 terminator can have a significant impact on the expression of transgenes (F de Felippes et al.
186 2020; P.-H. Wang et al. 2020).
187 While the correlation between terminator strength and gene expression was low, we
188 wondered whether the function of a gene and the strength of its terminator were more
189 correlated. To address this question, we performed gene ontology (GO) term enrichment
190 analysis on the genes associated with the strongest 10% of terminators from *Arabidopsis* or
191 maize. For both species, we found a significant enrichment (adjusted p value < 0.05) for genes
192 related to metabolism and response to stimulus (Supplementary Fig. 5a-d). Terminators derived
193 from oxidoreductase-related and stress-responsive genes in *Arabidopsis* were overrepresented

194 in the top 10% of terminators ranked by strength in tobacco leaves and maize protoplasts.
195 Maize terminators derived from genes involved in small molecule metabolic processes were
196 overrepresented in the strongest 10% of terminators in both systems. However, we found many
197 more significant GO terms associated with metabolism for the strongest maize terminators in
198 maize protoplasts than in tobacco leaves (Supplementary Fig. 5e, f). The latter finding pointed
199 to possible species-specific differences in terminator strength, prompting us to investigate this
200 possibility further.

201 Plant terminator strength is species-specific

202 mRNA 3' end processing may differ between monocotyledonous and dicotyledonous
203 plants, as suggested from studies in the 1980s. For example, the gene encoding the small
204 subunit of ribulose 1,5-bisphosphate carboxylase (*rbcS*) from the monocot wheat is improperly
205 polyadenylated when tested in the dicot tobacco (Keith and Chua 1986). In contrast, the mRNA
206 of the *rbcS* gene from the dicot pea is efficiently polyadenylated in tobacco (Nagy et al. 1985).
207 Consistent with these earlier findings, we observed a relatively weak correlation (R^2 = 0.33)
208 between the strength of a given terminator in the dicot model tobacco leaves versus the
209 monocot model maize protoplasts (Fig. 2a). In tobacco leaves, terminators from the dicot
210 *Arabidopsis* performed significantly better than terminators from the monocot maize. Similarly, in
211 maize protoplasts, maize terminator sequences significantly outperformed *Arabidopsis*
212 terminators (Fig. 2b, c). These observations are consistent with species-specific differences in
213 plant terminator strength.
214 Based on these observations, we wanted to identify terminators with strong species-
215 specific activity. Since our assay systems show different dynamic ranges, we normalized
216 terminator strength within each assay system to a scale from 0 (weakest) to 1 (strongest). We
217 defined a variable Ψ as the difference between the normalized terminator strength in tobacco
218 leaves and in maize protoplasts, such that a high Ψ value denotes a terminator that was
219 considerably stronger in tobacco leaves than in maize protoplasts. We found that *Arabidopsis*
220 terminators show a higher average Ψ value than maize terminators (Fig. 2d). We selected the
221 top 10% of *Arabidopsis* terminators (n = 1,923) with highest Ψ values, *i.e.* tobacco-specific
222 strength, and the top 10% of maize terminators (n = 2,439) with the lowest Ψ values, *i.e.* maize-
223 specific strength, for GO term enrichment analysis. *Arabidopsis* terminators with highly tobacco-
224 specific strength tended to be derived from stimulus- and stress-responsive genes, while maize
225 terminators with highly maize-specific strength tended to be derived from metabolic genes (Fig.
226 2e).
227 To understand how species-specific terminator strength is mediated, we used STREME
228 (Bailey 2021) to search for RNA motifs that were enriched in the tobacco-specific *Arabidopsis*
229 terminators (high Ψ) relative to the maize-specific maize terminators (low Ψ), and *vice versa*.
230 The most enriched motifs in the tobacco-specific *Arabidopsis* terminators were dominated by
231 long stretches of U nucleotides, while the most enriched motifs found in maize-specific maize
232 terminators favored G and C nucleotides (Fig. 2f, g). These findings motivated us to further
233 analyze the effect of nucleotide composition on terminator strength.

234 Nucleotide composition affects terminator strength in a position-specific manner

235 Dicot genomes have a lower GC content than monocot genomes (Singh, Ming, and Yu
236 2016). This bias also holds true for *Arabidopsis* and maize terminator sequences (Fig. 3a).
237 Assessing the impact of GC content on terminator strength, we found that terminators with
238 either high or low GC content were weaker than those with intermediate GC content in both
239 tobacco leaves and maize protoplasts (Fig. 3b, c). There are, however, subtle differences
240 between the two assay systems. In tobacco leaves, terminators with a GC content around 30-

35% were the strongest, while in maize protoplasts, terminators with a GC content of approximately 35-40% were the strongest. To substantiate these subtle differences, we measured the terminator strength of random sequences with a GC content of 30%, 40%, 50%, 60%, or 70%. In tobacco leaves, the random sequences with a GC content of 30% performed best, while in maize protoplasts, the random sequences with a GC content of 40% showed the highest strength (Supplementary Fig. 6). These values coincide with the average GC content of *Arabidopsis* terminators (32.5%; the average GC content of tobacco terminators is likely in a similar range) and maize terminators (40.9%). Thus, we conclude that the cleavage and polyadenylation machinery is likely attuned to the species-specific GC content of plant terminators.

Since terminator strength is governed at the RNA level, G and C or A and U nucleotides are not necessarily represented equally. Therefore, we teased apart the positional effect on terminator strength for each of the four nucleotides (Fig. 3d, e). We found that C nucleotides have little to no effect on terminator strength in tobacco leaves or maize protoplasts. High G content was beneficial at the 5' end of our tested sequences but not tolerated near the cleavage site, especially in tobacco leaves. Conversely, high U content near the 5' end was associated with lower terminator strength. The system preferences diverged, however, for sequences with high U content starting from 100 nucleotides upstream from the cleavage site: U-rich sequences in this region were associated with increased terminator strength in tobacco leaves but not in maize protoplasts. High A content around 20 nucleotides upstream of the cleavage site was correlated with terminator strength in both systems, probably due to the canonical polyadenylation signal — a short sequence often represented by the hexamer AAUAAA — typically found at this location.

Canonical cleavage and polyadenylation motifs contribute to terminator strength

Since the strength of a terminator is only partially explained by its nucleotide composition, we searched for sequence motifs that contribute to terminator strength. To this end, we conducted a motif enrichment analysis on the strongest 25% of terminators in both assay systems. The most significantly enriched motifs match canonical cleavage and polyadenylation signals: the UGUA sequence motif from the Far Upstream Element (FUE) and the AAUAAA polyadenylation signal (Fig. 4a). While these motifs are known to affect cleavage and polyadenylation, our assay allowed us to determine the quantitative contribution of each motif to terminator strength.

The UGUA motif is highly prevalent in our library, with 60% to 80% (small differences between the UGUA-containing motifs identified by STREME lead to different numbers of positive terminators) of all terminators containing this motif. The UGUA motif is predominantly located 30 to 40 nucleotides upstream of the cleavage site in both *Arabidopsis* and maize terminators (Supplementary Fig. 7a, b). In tobacco leaves and maize protoplasts respectively, terminators with a UGUA motif were on average 50% and 20% stronger than those without this motif (Fig. 4b, c). Consistent with prior reports (Rothnie, Reid, and Hohn 1994), the number of UGUA motifs also correlates with terminator strength and cleavage probability (Supplementary Fig. 8e, f).

The polyadenylation signal is less prevalent in our library (15% to 35% of all terminators) but shows a distinct localization profile, with a sharp peak about 20 nucleotides upstream of the cleavage site (Supplementary Fig. 7c, d). The polyadenylation signal contributes significantly to terminator strength. In tobacco leaves and maize protoplasts respectively, terminators with a polyadenylation motif were 40% and 20% stronger than those without this motif (Fig. 4b, c). Since fewer than half of the terminators in our library contain a canonical polyadenylation signal, we asked if similar sequences are functionally equivalent. Terminators with a perfect AAUAAA

290 sequence were stronger than terminators with a sequence that differs by a single nucleotide
291 (carrying a single-nucleotide variant of this motif), although AAUAAG and AAUAAU motifs
292 performed nearly as well. Terminators without any AAUAAA-like sequence were considerably
293 weaker (Supplementary Fig. 8a, b).
294 In addition to the AAUAAA and UGUA motifs (A. G. Hunt 1994; F. de Felippes and
295 Waterhouse 2023), we found novel U- and G-rich motifs enriched in the strongest terminators
296 (Fig. 4a). These U/G-rich motifs are broadly distributed upstream of the polyadenylation signal
297 and at slightly higher frequency just upstream or downstream of the cleavage site
298 (Supplementary Fig. 7e, f). While the U/G-rich motifs share a similar localization pattern, there
299 are striking differences between the motifs discovered in the tobacco leaf and the maize
300 protoplast system. The motif detected in the tobacco leaf data is found in nearly 90% of all
301 terminators and consists of a G nucleotide surrounded by 2 to 3 U nucleotides. In contrast, the
302 motif identified in the maize protoplast data is much less prevalent (16% of all terminators) and
303 consists of alternating U and G nucleotides (Fig. 4a). Despite these differences, both motifs
304 have an influence on terminator strength, leading to a 40% and 20% increase in strength for
305 terminators with the motif as compared to those without, in tobacco and maize respectively (Fig.
306 4b, c).
307 While each individual motif contributes positively to terminator strength, we observed
308 additive effects when multiple motifs are present within the same terminator. Independent of the
309 assay system, the strongest terminators contain all three motifs and were on average 60% more
310 active than terminators without any motifs (Fig. 4d, e). To validate the effect of the identified
311 AAUAAA and UGUA motifs on terminator strength, we selected 20 terminators each with a
312 single strong AAUAAA or UGUA motif and generated single or double nucleotide mutations to
313 break the motif. The terminator strength of the original and mutated sequences was then
314 measured in tobacco leaves and maize protoplasts. Most motif mutations lowered terminator
315 strength (Supplementary Fig. 8c, d). Mutations in the AAUAAA motif caused, on average, a 24%
316 decrease in terminator strength in tobacco leaves and a 16% decrease in maize protoplasts.
317 Mutations in the UGUA motif decreased terminator strength by approximately 13% and 7% in
318 tobacco leaves and maize protoplasts, respectively.
319 Next, we wondered if we could use the enriched motifs to improve the strength of weak
320 terminators. We selected randomized sequences from our initial data that showed low
321 terminator strength and did not contain an AAUAAA, a UGUA, or a U/G-rich motif. We then
322 inserted a CA dinucleotide at the predicted cleavage site (position 150) and added all possible
323 single, double, and triple combinations of the AAUAAA, UGUA, and U/G-rich motifs. All
324 sequences were then subjected to Plant STARR-seq in tobacco leaves and maize protoplasts.
325 In most cases, adding motifs increased terminator strength and additive effects were observed
326 when multiple motifs were inserted into a terminator (Fig. 4f, g). On average, single motifs led to
327 a 5% to 20% increase in terminator strength. Terminators with all three motifs were
328 approximately 60% stronger than motif-less terminators in tobacco leaves and maize
329 protoplasts. Although the GUGUG motif was originally identified in data from the maize
330 protoplast system, it also increased terminator activity in tobacco leaves. Taken together, these
331 findings demonstrate that the motifs enriched in strong terminators are indeed contributing to
332 terminator strength.

333 Computational models accurately predict terminator strength

334 Computational models can successfully predict the activity of regulatory elements by
335 learning key sequence features (Cuperus et al. 2017; Griesemer et al. 2021; Jores et al. 2021).
336 To develop computational models that can predict terminator strength, we initially focused on
337 using k-mer counts as a proxy for terminator activity. To test the validity of this approach, we
338 counted the occurrence of all possible 6-mers (4,096 sequences) in the terminator sequences,

339 and calculated the correlation between terminator strength and how often a given 6-mer was
340 represented in a terminator sequence. As expected, we found that the 6-mers most correlated
341 with terminator strength in tobacco leaves and maize protoplasts are variations of the canonical
342 cleavage and polyadenylation signals AAUAAA and UGUA (Fig. 5a, b). However, we observed
343 only a moderate conservation of the 6-mer rank orders between the two assay systems
344 (Spearman's ρ = 0.29; Fig. 5c). 6-mers that were highly correlated with terminator strength in
345 tobacco leaves but not in maize protoplasts were U-rich. Conversely, 6-mers with a high
346 correlation to terminator strength in maize protoplasts but not in tobacco leaves were rich in G
347 and C nucleotides (Fig. 5c, d). These findings are consistent with our prior observations on
348 sequence motifs associated with high terminator activity, both within and across the two assay
349 systems. Therefore, we used 6-mer counts as input features to train a lasso regression model to
350 predict terminator strength. The model was trained on 70% of our terminator data and tested on
351 30% of the data. The lasso regression model had moderate predictive power, explaining 28% of
352 the variance in terminator strength in tobacco leaves and 41% in maize protoplasts (Fig. 5e, f).
353 To build a model with increased predictive power, we turned to a convolutional neural
354 network with a DenseNet architecture (Huang et al. 2017), because this approach had worked
355 well with Plant STARR-seq data previously (Deng et al. 2023). Our DenseNet model uses the
356 sequence of a terminator as an input and predicts the strength of this sequence in tobacco
357 leaves and maize protoplasts. After the model was trained on 90% of the terminator data, it
358 could accurately predict terminator strength for the remaining 10% of the data. The features
359 learned by the model explained 76% and 67% of the variance in terminator strength in tobacco
360 leaves and maize protoplasts, respectively (Fig. 6a, b). To understand what features the
361 DenseNet model had learned, we used DeepLIFT and TF-MoDISco to extract consolidated
362 sequence motifs that positively or negatively impact terminator strength (Shrikumar, Greenside,
363 and Kundaje 2017; Shrikumar et al. 2018) prediction (Fig. 6c-f). According to this analysis,
364 AAUAAA and UGUA motifs are associated with increased terminator strength in both assay
365 systems. U-rich sequences decrease terminator strength in maize protoplasts, especially if they
366 surround a UGUA motif. In contrast, U-rich sequences increase terminator strength in tobacco
367 leaves, although this effect can be reversed by GG dinucleotides (Fig. 6e, f). These findings are
368 consistent with the results from our motif enrichment and k-mer analyses and indicate that the
369 DenseNet model has learned biologically relevant terminator features.
370

371 ## *In silico* evolution of terminator sequences

372 While our previous attempts to improve terminator strength by adding polyadenylation
373 and cleavage motifs were successful, the gain in terminator strength was modest (Fig. 4f, g). *In*
374 *silico* evolution using convolutional neural network models can drastically improve the activity of
375 regulatory elements (Cuperus et al. 2017; Jores et al. 2021). Therefore, we used our DenseNet
376 model for *in silico* evolution of 222 terminators, 111 each from *Arabidopsis* and maize. As
377 starting sequences, we randomly selected terminators from the held-out test set used to validate
378 the DenseNet model. For each terminator, we generated every possible single-nucleotide
379 substitution variant and scored these variants with the DenseNet model. We kept the variant
380 with the highest predicted terminator strength and subjected it to another round of evolution for
381 a maximum of ten rounds (Fig. 7a). We performed this process three times using the prediction
382 for either tobacco leaves or maize protoplasts, or the sum of both predictions to identify the
383 strongest variant. To test the evolved elements experimentally, we synthesized the starting
384 sequences and those obtained after three and ten rounds of evolution, and experimentally
385 assayed their terminator strength in tobacco leaves and maize protoplasts.
386 After three rounds of evolution (*i.e.*, after changing only three nucleotides), terminator
387 strength increased, on average, 5-fold in tobacco leaves and 1.6-fold in maize protoplasts (Fig.

388 7b, c). For sequences obtained after ten rounds of evolution, a further increase in terminator
389 strength was observed. Even though the original sequences and those obtained after *in silico*
390 evolution differed by only ten nucleotides, the difference in their terminator strength was 12-fold
391 in tobacco leaves and 4-fold in maize protoplasts (Fig. 7b, c). As expected, the increase in
392 terminator strength was most pronounced when the prediction used to score variants during *in*
393 *silico* evolution matched the experimental assay system (*i.e.* using the tobacco leaf prediction
394 for evolution, and testing the resulting terminators in tobacco leaves). Although all starting
395 sequences were weaker than the 35S terminator, our *in silico* evolution approach generated
396 several terminators of greater strength than this highly active viral terminator (Fig. 7b, c). We
397 tested selected evolved terminators with the dual-luciferase assay and found strong
398 correspondence with the Plant STARR-seq results (Fig. 7d, e). Furthermore, we observed that
399 the model favored the insertion of multiple UGUA motifs into the evolved, stronger terminators
400 (Supplementary Fig. 8g).
401

402 ## Cleavage and polyadenylation efficiency affects terminator strength

403 Over 70% of the genes in *Arabidopsis* and maize contain more than one possible
404 polyadenylation site and can therefore give rise to transcript isoforms that differ in 3' UTR length
405 (Jafar et al. 2019; Wu et al. 2011). Alternative polyadenylation can have a strong effect on
406 transcript levels through the inclusion or exclusion of regulatory features such as binding sites
407 for microRNAs or RNA-binding proteins (Bernardes and Menossi 2020). We wondered whether
408 the terminator strength of putative polyadenylation sites affects the choice of which site is used.
409 To address this question, we measured the terminator strength of primary and secondary
410 cleavage and polyadenylation sites from over 5000 genes. However, there was no difference
411 between the terminator strength of primary and secondary polyadenylation sites for *Arabidopsis*
412 or maize terminators (Supplementary Fig. 9).
413 While terminator strength could not predict which potential polyadenylation site is more
414 likely to be used in a genomic context, we wondered if the reverse were true: Is the strength of a
415 terminator associated with the efficiency of its cleavage and polyadenylation? To determine the
416 cleavage and polyadenylation sites in our terminators, we subjected the output RNA from a
417 Plant STARR-seq experiment in tobacco leaves to 3' end sequencing (Fig. 8a). We defined the
418 cleavage and polyadenylation sites for each terminator as local maxima in the distribution of the
419 cleavage positions along the terminator sequence for all unique reads. As expected, the vast
420 majority of the cleavage and polyadenylation sites identified by this approach coincided with a
421 CA or UA dinucleotide (Fig. 8b) matching the known cleavage element (A. G. Hunt 1994; Loke
422 et al. 2005). Consistent with prior reports (Rothnie, Reid, and Hohn 1994; Mogen et al. 1992;
423 Sanfaçon, Brodmann, and Hohn 1991; Mogen et al. 1990) we observed near complete cleavage
424 of the 35S terminator with one major cleavage site at the same position as previously shown
425 (Supplementary Fig. 10b). We confirmed the cleavage pattern of several terminators with RT-
426 PCR and gel electrophoresis (Supplementary Fig. 10c).
427 The terminators in our library were designed to contain a cleavage site at position 150
428 (Fig. 1a). About 61% of the terminators showed a cleavage site within 5 nucleotides upstream or
429 downstream of this position, and for approximately half of these (32% of all terminators), this
430 was the primary cleavage site (Table 1). Of the 54,825 terminators for which we could call
431 cleavage sites, 68% had more than one cleavage sites, and of those, 20% (about 13% of all
432 terminators) had a prominent secondary cleavage site indicated by at least 30% of the reads
433 (Table 1; see Fig. 8c for examples). However, 17% of the tested sequences were not cleaved
434 and polyadenylated but showed read-through into the downstream T-DNA sequence.
435 We observed differences in the cleavage pattern between *bona fide* terminators and control
436 sequences (Fig. 8d, Table 1). Plant terminators were predominantly cleaved at position 150. In

437 contrast, randomized sequences showed a broad distribution of cleavage sites throughout their
438 sequence. However, for the positional random sequences which resemble terminators more
439 closely than the global random controls, the distribution was shifted towards an enrichment of
440 cleavage at or near position 150. Finally, control sequences derived from coding regions were
441 rarely cleaved and polyadenylated, consistent with a selection against potential cleavage sites.
442 These general trends held true when considering all cleavage sites, in addition to primary sites
443 (Supplementary Fig. 10a).
444 Next, we tested the association of terminator strength and cleavage probability (*i.e.*, the
445 likelihood of a terminator being cleaved and polyadenylated instead of allowing read-through
446 transcription). Cleavage probability was strongly correlated with terminator strength (Fig. 8e, h),
447 and terminators with a primary cleavage site within their sequence were approximately 40%
448 stronger than those without (Fig. 8g). Furthermore, terminators with a dominant cleavage site
449 (*i.e.*, most transcripts are cleaved at this site) were stronger terminators than those with multiple
450 weak cleavage sites (Fig. 8f). Taken together, the efficiency and accuracy with which a
451 terminator is cleaved and polyadenylated determines its strength. Strong terminators show a
452 dominant cleavage site and prevent read-through into downstream sequences.

453 ## Polyadenylation motifs and GC content control cleavage probability

454 Since cleavage probability and terminator strength were positively correlated, we asked
455 if the same features that influence terminator strength also affect cleavage probability. First, we
456 tested if biological terminator function was associated with a high cleavage probability. Indeed,
457 plant terminators showed a much higher cleavage probability than control sequences from
458 coding regions (Fig. 9a). Randomized control sequences with a nucleotide composition similar
459 to an average terminator were also significantly more likely to be cleaved and polyadenylated
460 than the coding region controls, but their average cleavage probability was still lower than that
461 of *bona fide* plant terminators. The cleavage probability for sequences derived from *Arabidopsis*
462 was higher than the one for maize sequences (Fig. 9a).
463 As GC content is one of the key differences between terminators from *Arabidopsis* and
464 maize, we asked if cleavage probability was affected by GC content. We observed a strong
465 negative correlation (Pearson's r = -0.65) between these two factors. While a high AT content
466 was associated with a high cleavage probability, increasing GC content led to decreased
467 cleavage probability (Fig. 9b). This finding likely explains why maize sequences, which show on
468 average an approximately 10% higher GC content than *Arabidopsis* sequences, were less likely
469 to be cleaved than *Arabidopsis* sequences. Our observation that AU-rich sequences show high
470 cleavage probability is consistent with previous reports that the insertion of AU-rich sequences
471 into transcripts can lead to their cleavage and polyadenylation in maize (Luehrsen and Walbot
472 1994). Although both terminator strength and cleavage probability were affected by GC content,
473 they followed different trends. Cleavage probability decreased monotonically with increasing GC
474 content, while terminator strength was highest at an intermediate GC content and lowest in very
475 AT- or GC-rich sequences (Fig. 3b, c). Similarly, we observed differing and position-specific
476 effects of local nucleotide composition on terminator strength, whereas for cleavage probability,
477 positional effects were much less pronounced, and A and T nucleotides behaved mostly similar
478 to each other as did G and C nucleotides (Fig. 9c).
479 Finally, we tested if the AAUAAA, UGUA and U/G-rich motifs affected cleavage
480 probability. While all three motifs increased cleavage probability, the AAUAAA motif clearly had
481 the largest effect (Fig. 9d). As for terminator strength, we observed additive effects of the motifs
482 on cleavage probability, and terminators with all three motifs were most likely to be cleaved and
483 polyadenylated.

Discussion

Here, we adapted Plant STARR-seq to characterize and optimize plant terminator sequences. We find that thousands of *Arabidopsis* and maize terminators outperformed the commonly used bacterial NOS and MAS terminators; a handful even outperformed the viral 35S terminator. These results provide a large arsenal of diverse and strong plant terminators to use with transgenes, which should alleviate transgene silencing (Diamos and Mason 2018) . The optimal terminators to employ in constructing transgenes may be those with high cleavage probability, as these prevent the read-through transcription implicated in silencing (F de Felippes et al. 2020). Thus, for use in dicots, good terminators to choose would be those from the *Arabidopsis* genes AT3G46230 (HEAT SHOCK PROTEIN 17.4), AT2G05530, and AT4G39730 (PLAT DOMAIN PROTEIN 1); for use in monocots, good ones would be those from the maize genes Zm00001d016542 (anthranilate 1,2-dioxygenase), Zm00001d047961, and Zm00001d017119 (glucose-6-phosphate dehydrogenase 5).

In addition to these naturally occurring terminators, *in silico* evolved, synthetic terminator sequences — several of which showed greater strength and higher reporter protein abundance than the viral 35S terminator — resulted from this work. Use of the DenseNet prediction that best matched the assay system (the tobacco leaf prediction for dicots, and the maize protoplast prediction for monocots) led to the best results; however, a combination of both predictions can generate terminators that are active across a broad range of plant species, tissues, and applications. The iterative *in silico* evolution and testing of evolved elements in Plant STARR-seq appears to be a promising generalizable path toward improving the features of plant regulatory elements, as for core promoters (Jores et al. 2021; Jores et al. 2023).

Beyond the practical benefits of this study, we identified novel features of terminator biology in plants. We found that GC content profoundly influences terminator strength and cleavage probability in different ways. The strongest terminators had a GC content of approximately 30 – 40% (depending on the assay system), with terminator strength lowest at either higher or lower GC percentage in both assay systems. In contrast, cleavage probability monotonically decreased with increasing GC content in tobacco leaves (and was not measured in maize protoplasts due to technical challenges). This negative correlation is similar to the effects of GC content on core promoter strength, which shows a strong negative correlation with GC content in tobacco leaves but not in maize protoplasts (Jores et al. 2021). Taken together, GC content appears to affect different regulatory elements in different ways, and these effects vary across species, reflecting genomic GC content.

In addition to known polyadenylation motifs (A. G. Hunt 1994; Bernardes and Menossi 2020; Felipe F. de Felippes and Waterhouse 2023), we discovered novel motifs that increased terminator strength and cleavage probability. These motifs are rich in U and G nucleotides and reside broadly across terminator sequences, with a moderate enrichment immediately upstream and downstream of the cleavage site. The precise composition of these U/G-rich motifs differed between the tobacco leaf and the maize protoplast systems; however, the maize-specific motif also contributed to terminator strength in tobacco leaves. Human terminators contain a GU-rich element downstream of the cleavage site that is required for efficient polyadenylation and that is bound by the cleavage-stimulating factor (CSTF) complex (Beyer, Dandekar, and Keller 1997; Takagaki and Manley 1997; B. Tian and Graber 2012). Plant homologs for members of the CSTF complex can form a similar complex and bind to RNA (Arthur G. Hunt, Xing, and Li 2012; Yao et al. 2002; Bell and Hunt 2010). We speculate that the novel U/G-rich motifs identified here serve as binding sites for the plant CSTF complex.

The assay design employed here provided insight into cleavage probability and alternative polyadenylation. Alternative polyadenylation is a crucial mechanism to create diverse transcripts in response to environmental change and in particular tissues (Bernardes and Menossi 2020; Wu et al. 2011; Ye et al. 2019). Alternative polyadenylation produces transcripts

534 with altered 3' UTR length, resulting in different mRNAs and translation levels. Long 3' UTRs
535 decrease transcript stability by triggering nonsense-mediated mRNA decay (Kertesz et al.
536 2006), while short 3' UTRs make translation more efficient by promoting polysome formation
537 (Chang et al. 2015). When we compared the 170 nucleotide-terminator sequences of
538 *Arabidopsis* and maize genes derived from primary vs. secondary polyadenylation sites, we
539 observed no difference in terminator strength among sites derived from *Arabidopsis* or maize.
540 These comparisons suggest that the sequence surrounding a given polyadenylation site does
541 not fully explain alternative polyadenylation. T*rans*-acting factors such as the components of the
542 cleavage and polyadenylation complexes, RNA-binding proteins and non-coding RNAs are
543 involved in the choice of polyadenylation sites, presumably by recognizing sequence context
544 and secondary structure of the entire terminator sequence instead of the shorter terminator
545 sequences tested here (Zhang et al. 2020; Arthur G. Hunt 2022; Bernardes and Menossi 2020).
546 A comparison of all tested terminator sequences indicates that strong terminators tended to
547 contain a dominant cleavage site rather than multiple weaker ones.
548

549 # Methods

550 ## Library Design and Construction

551 For this study, we defined terminators as the sequence from 150 nucleotides upstream
552 to 20 nucleotides downstream of a cleavage and polyadenylation site. For *Arabidopsis*, we used
553 experimentally determined cleavage and polyadenylation sites described by Thomas *et al.*
554 *(Thomas et al. 2012)*. We selected the primary cleavage and polyadenylation sites for each
555 gene (n = 18,450) in wild-type plants, as well as prominent secondary cleavage sites that had at
556 least 30% of total reads per gene (n = 2,325). For the 3,754 genes without an experimentally
557 defined cleavage site, we utilized the end of their 3' UTR annotation in the *Arabidopsis* TAIR10
558 annotation as the cleavage site. This yielded a total of 24,529 *Arabidopsis* terminator sequences
559 (Supplementary Table 1). For maize, we used cleavage and polyadenylation sites defined by
560 Jafar *et al. (Jafar et al. 2019)*. We selected primary cleavage sites for 25,685 maize genes, and
561 included 4,407 secondary cleavage sites (at least 30% of total reads per gene) for a total of
562 30,092 maize terminator sequences (Supplementary Table 1).
563 In addition to *bona fide* terminators, several control sequences were added to the library
564 (Supplementary Table 1). Since protein coding sequences should not contain cleavage and
565 polyadenylation motifs, 170-nucleotide long sequences (589 each from *Arabidopsis* and maize)
566 from coding regions with a similar GC content as the terminator library were included as
567 negative controls. Furthermore, we generated random sequences with global (200 sequences
568 per species) or position-specific (1,000 sequences per species) nucleotide frequencies derived
569 from the average *Arabidopsis* or maize terminator. Randomized sequences with a GC content
570 of 30%, 40%, 50%, 60%, or 70% (200 sequences of 170 nucleotides each) were added to test
571 effects of GC content on terminator strength. Finally, four commonly used non-plant terminators
572 (t35S, tAg7, tNOS, and tMAS) were added as a frame of reference in their full length (35S=204
573 nt, Ag7=208 nt, MAS= 253 nt, NOS=253 nt). The final library of sequences was ordered as an
574 oligo pool from Twist Biosciences (Supplementary Table 2).
575 To validate and extend our findings from the large-scale terminator library, we created a
576 second, smaller library. This library included 187 terminators from the original library to test the
577 correlation between results from the two libraries. Additionally, we added sequences to validate
578 the importance of the discovered motifs. We picked 20 sequences from the randomized control
579 sequences in our original library that had neither a CA dinucleotide at the predicted cleavage
580 site, nor an AAUAAA, a UGUA, or a GUGUG motif. For each validation sequence, we added a

581 CA dinucleotide at position 150 and all possible combinations of these three motifs at the
582 positions where they are found most often in our library. To test the importance of the AAUAAA
583 motif, we picked twenty terminators that had only one AAUAAA sequence and generated three
584 variants with a mutation in this sequence (ACTCAA, ACTCAA, ACTAAA). Similarly, we took
585 twenty sequences that had only one UGUA sequence and replaced it with mutated variants
586 (UGCA, CGUA, UCUA). Finally, we included the sequences from the *in silico* evolution (see
587 below) in this validation library (Supplementary Table 3).
588 The Plant STARR-seq plasmid pPSt (https://www.addgene.org/203590/) used in this
589 study is based on the pPSup plasmid (https://www.addgene.org/149416/) (Jores et al. 2020)
590 with adaptations to enable the characterization of terminators. The base plasmid pPSt contains
591 three consecutive Golden Gate cloning sites. To generate the terminator libraries, we first
592 inserted the 35S promoter together with a 5' UTR derived from the maize histone H3 gene
593 Zm00001d041672, an ATG start codon, and a 18-nucleotide random barcode
594 (VNNVNNVNNVNNVNN; V = A, C or G) into the upstream Golden Gate site using the restriction
595 enzyme BbsI-HF (NEB). Next, we cloned the array-synthesized terminator library into the
596 downstream Golden Gate site using the restriction enzyme Esp3I (NEB). In this step, the
597 plasmid library was bottlenecked to approximately 1,000,000 variants (approximately 16
598 barcodes per terminator) or 60,000 variants (approximately 30 barcodes per terminator) for the
599 large-scale or the validation library, respectively. Finally, we used BsaI-HFv2 (NEB) to replace
600 the central Golden Gate site with the coding sequence of GFP lacking the start codon. Two
601 versions of the library were created in this step: one with full-length GFP for use in Plant
602 STARR-seq (see https://www.addgene.org/203592/ for an example of a fully assembled Plant
603 STARR-seq plasmid with the 35S terminator.) and one with a truncated version of GFP lacking
604 the central 188 amino acids for subassembly (see below). The sequences of all primers used for
605 cloning and sequencing are included in Supplementary Table 4.
606

607 ## Tobacco cultivation and transformation

608 Tobacco (*Nicotiana benthamiana*) was grown in soil (Sunshine Mix no. 4) at 25°C with a
609 long day photoperiod (16 h light and 8 h dark; cool-white fluorescent lights Philips TL-D
610 58 W/840; intensity 300 µmol m^{-2} s^{-1}). Plants were transformed approximately 3 weeks after
611 germination. The *Agrobacterium* transformation and induction method was previously described
612 (Jores et al. 2021). The terminator libraries were introduced into *Agrobacterium tumefaciens*
613 strain GV3101 (harboring the virulence plasmid pMP90 and the helper plasmid pMisoG) by
614 electroporation. *Agrobacterium* cultures were infiltrated into the first two mature leaves of
615 tobacco plants (12 plants/24 leaves per replicate for the large-scale library; 3 plants/6 leaves for
616 the smaller validation library). The plants were further grown for 48 hours under normal light
617 conditions before mRNA extraction. The input sample for Plant STARR-seq was obtained from
618 20 mL of the *Agrobacterium* solution that was used to infiltrate tobacco leaves. To this end, the
619 QIAprep Spin Miniprep Kit was used according to the manufacturer's instructions.
620

621 ## Maize mesophyll protoplast generation and PEG transformation

622 We used the PEG transformation method of maize mesophyll protoplasts as described in
623 (Tonnies et al. 2023). Maize (Zea mays L. cultivar B73) seeds were soaked in water overnight at
624 25°C. The seeds were germinated in soil for 3 days under long day conditions (16 hours light, 8
625 hours dark) at 25°C, then moved to complete darkness at 25°C for 10-11 days. From each
626 seedling, 10 cm sections from the second and third leaf were cut into thin 0.5 mm strips
627 perpendicular to veins and immediately submerged in 10 ml of protoplasting enzyme solution

628 (0.6 M mannitol, 10 mM MES ph 5.7, 15 mg/ml cellulase R10, 3 mg/ml macerozyme, 1 mM
629 CaCl2, 0.1% [w/v] BSA, and 5 mM beta-mercaptoethanol). The mixture was covered in foil to
630 keep out light, vacuum infiltrated for 3 min at room temperature (RT), and incubated on a shaker
631 at 40 rpm for 2.5 hours at RT. Protoplasts were released by incubating an extra 10 min at 80
632 rpm. To quench the reaction, 10 mL ice-cold MMG (0.6 M Mannitol, 4 mM MES ph 5.7, 15 mM
633 MgCl2) was added to the enzyme solution and the whole solution was filtered through a 40 µM
634 cell strainer. To pellet protoplasts, the filtrate was split into equal volumes of no more than 10
635 mL in chilled round-bottom glass centrifuge vials and centrifuged at 100 x g for 4 min at RT.
636 Pellets were resuspended in 1 mL cold MMG each and combined into a single round-bottom
637 vial. To wash, MMG was added to make a total volume of 5 mL and the solution was centrifuged
638 at 100 x g for 3 min at RT. This wash step was repeated two more times. The final pellet was
639 resuspended in 1-2 mL of MMG. A sample of the resuspended protoplasts was diluted 1:20 in
640 MMG and used to count the number of viable cells using Fluorescein Diacetate as a dye.
641 For each replicate, 20 million protoplasts were mixed with 200 µg of the terminator plasmid
642 library in a fresh tube, topped with MMG to a volume of 2,288 µL, and incubated on ice for 30
643 min. For PEG transformation, 2,112 µL of PEG solution (0.6 M Mannitol, 0.1 M CaCl2, 25%
644 [w/v] poly-ethylene glycol MW 4000) was added to reach a final concentration of 12% (w/v)
645 PEG. The mixture was incubated for 10 min in the dark at RT. After incubation, the
646 transformation solution was diluted with 22 mL (5 x 4.4 mL) incubation solution (0.6 M Mannitol,
647 4 mM MES pH 5.7, 4 mM KCl), and centrifuged at 100 x g for 4 min at RT. For the PEG
648 transformation with the validation library, we used 4 million protoplasts, 40 µg of the plasmid
649 library, and one fifth of the buffer volumes used for the large-scale library.
650 After transformation, the protoplast pellet was washed with 5 mL of incubation solution,
651 centrifuged at 100 x g for 3 min at RT, and resuspended in incubation solution to a
652 concentration of 500 cells/µL. Protoplasts were incubated overnight in the dark at RT to allow for
653 transcription of the plasmid library and then pelleted (4 min, 100 x g, RT). The pellet was
654 washed with 5 mL incubation solution and centrifuged (3 min, 100 x g, RT). The pellet was
655 finally resuspended in 5 mL incubation solution. An aliquot of the solution was used to check
656 transformation efficiency under a microscope (12.4% [replicate 1] and 49.5% [replicate 2]
657 transformation efficiency for the large-scale library; 62% [replicate 1] and 45% [replicate 2] for
658 the validation library). Cells were pelleted (4 min, 100 x g, RT) and resuspended in 2 mL Trizol
659 for subsequent mRNA extraction. An aliquot of the plasmid library used for PEG transformation
660 was used as the input sample for Plant STARR-seq.

661 ## Plant STARR-seq assay

662 For all Plant STARR-seq experiments, two independent biological replicates were
663 performed. Different plants and fresh *Agrobacterium* cultures were used for each biological
664 replicate.
665 Tobacco leaves were harvested 2 days after infiltration and partitioned into batches of 4 (large-
666 scale library) or 3 (validation library) leaves. The leaf batches were frozen in liquid nitrogen,
667 finely ground with mortar and pestle, and immediately resuspended in 12 mL Trizol. The
668 suspensions were cleared by centrifugation (5 min, 4,000 x g, 4°C) and each supernatant was
669 mixed with 2.5 mL chloroform. After centrifugation (15 min, 4,000 x g, 4°C), 7 mL of the upper,
670 aqueous phase was transferred to a new tube, and mixed by inversion with 3.5 mL high salt
671 buffer (0.8 M sodium citrate, 1.2 M NaCl) and 3.5 mL isopropanol. The solution was incubated
672 for 15 min at RT to precipitate the RNA and centrifuged (30 min, 4,000 x g, 4°C). The pellet was
673 washed in 10 mL ice-cold 70% ethanol, centrifuged (5 min, 4000 x g, 4°C), and air-dried. The
674 pellet was resuspended in 180 µL of warm (65°C) nuclease-free water and transferred to a new
675 tube. The solution was supplemented with 10 µL 20X DNase I buffer (1 mM CaCl2, 100 mM Tris
676 pH 7.4), 10 µL 200 mM MnCl2, 2µL DNase I (ThermoFisher Scientific), and 1 µL RNaseOUT

677 (ThermoFisher Scientific), and incubated for 30 min at 37°C. To precipitate the RNA, 20 µL 8M
678 ice-cold LiCl and 500 µL ice-cold 100% ethanol was added. After incubation for 15 min at -80°C,
679 the RNA was pelleted by centrifugation (20 min, 20,000 x g, 4°C). The pellet was washed with
680 500 µL ice-cold 70% ethanol, centrifuged (5 min, 20,000 x g, 4°C), air-dried for 10 min, and
681 resuspended in 200 µL nuclease-free water supplemented with 0.5 µL RNaseOUT. For cDNA
682 synthesis, eight reactions with 11 µL mRNA solution, 1 µL 2 µM GFP-specific reverse
683 transcription primer, and 1 µL 10 mM dNTPs were incubated at 65°C for 5 min then immediately
684 placed on ice. The reactions were supplemented with 4 µL 5X SuperScript IV buffer, 1 µL 100
685 mM DTT, 1 µL RNaseOUT, and 1 µL SuperScript IV reverse transcriptase (ThermoFisher
686 Scientific). To ensure that the samples were largely free of DNA contamination, four reactions
687 were used as controls, where the reverse transcriptase and RNaseOUT were replaced with
688 water. Reactions were incubated for 10 min at 55°C, followed by 10 min at 80°C. Sets of 4
689 reactions each were pooled. The cNDA was purified with the Zymo Clean&Concentrate-5 kit,
690 and eluted in 20 µL 10 mM Tris. The barcode was amplified with 10-20 cycles of polymerase
691 chain reaction (PCR) and read out by next generation sequencing.
692 For Plant STARR-seq in maize protoplasts, the protoplast-containing Trizol solution from PEG
693 transformation was transferred to 2 mL Phasemaker tubes (1 mL per tube; ThermoFisher
694 Scientific), mixed thoroughly with 300 µL chloroform, and centrifuged (5 min, 15,000 x g, 4°C).
695 RNA was extracted using the RNeasy Plant Mini Kit (QIAGEN). The supernatant was
696 transferred to a QIAshrededer column and centrifuged (2 min, 20,000 x g, RT). The flowthrough
697 was transferred to a new 1.5 mL tube and mixed with 300 µL 100% ethanol. Up to 500 µL of the
698 solution was loaded on an RNeasy mini spin column. After centrifugation (10 seconds, 16,100 x
699 g, RT) the flowthrough was discarded. This was repeated until all the solution had been added
700 to the column. The column was washed once with 700 µL RW1 buffer and twice with 500 µL
701 RPE buffer. After each wash step, the column was centrifuged (30 sec, 16,100 x g, RT) and the
702 flowthrough was discarded. The column was dried with an extra centrifugation step (30 sec,
703 16,100 x g, RT) and transferred to a 1.5 mL collection tube. For elution, 50 µL of RNase-free
704 water was added, and the column was incubated for 1 minute, and centrifuged (1 min, 16,100 x
705 g, RT). This elution step was repeated with an additional 40 µL of RNase-free water. The eluate
706 was treated with DNase I (5 µL of 20x DNaseI buffer, 5 µL 200 mM MnCL2, 1 µL RNaseOUT,
707 and 2 µL DNase I) for 1 h at 37°C. The solution was supplemented with 20 µL 500 mM EDTA,
708 1 µL 20 mg/mL glycogen, 12 µL ice-cold 8M LiCl, and 300 µL ice-cold 100% ethanol. The
709 solution was incubated 15 min at -80°C, centrifuged (20 min, 20,000 x g, 4°C). The pellet was
710 washed with 500 µL ice-cold 70% ethanol, and centrifuged (3 min, 20,000 x g, 4°C). The pellet
711 was air-dried for 10 min and resuspended in 100 µL RNase-free water. Reverse transcription,
712 purification, PCR amplification and sequencing were performed as for the tobacco samples.
713

714 ## Subassembly and barcode sequencing

715 Paired-end sequencing on an Illumina NextSeq 2000 platform was used to link
716 terminators to their respective barcodes. To facilitate sequencing, we created a shortened
717 version of the terminator library plasmid with a large deletion in the GFP gene. The terminator
718 region was sequenced using paired 151-nucleotide reads, and two 18-nucleotide indexing reads
719 were used to sequence the barcodes. The paired terminator and barcode reads were
720 assembled using PANDAseq (version 2.11) (Masella et al. 2012) and the terminator reads were
721 aligned to the designed terminator library using BowTie2 (version 2.4.1) (Langmead and
722 Salzberg 2012). Terminator-barcode pairs with less than 5 reads and terminators with a
723 mutation or truncation were discarded. For each Plant STARR-seq experiment, barcodes were
724 sequenced using paired-end reads on an Illumina NextSeq 2000 system. The paired barcode
725 reads were assembled using PANDAseq.

Computational methods

For calculating terminator strength, the reads for each barcode were counted in the input and cDNA (output) samples. Barcodes with less than five reads were discarded. For each terminator, the sum of the reads for all associated barcodes was calculated in the input and output samples. The input and output counts were normalized by dividing each by the sum of all counts in the output and input sample, respectively. Terminator strength was calculated as the normalized output counts divided by the normalized input counts. Terminator strength was normalized to the strength of the 35S terminator. We used the average terminator strength across two replicates for all analyses (Supplementary Tables 2 and 3). Spearman and Pearson's correlation were calculated using base R (version 4.3.0). Significance was calculated using the two-sided Wilcoxon rank-sum test and the ggsignif library (version 0.6.4) in R (Supplementary Table 5). GO term enrichment analysis was performed using the ggprofiler2 package (version 0.2.1) in R (Supplementary Table 6).

Discovery of terminator motifs

To find motifs enriched in strong terminators, we ranked terminators according to their strength in tobacco leaves or maize protoplasts. The sequences of the top 25% terminators were analyzed by STREME (version 5.5.1) (Bailey 2021) to find ungapped RNA motifs that are enriched in this set relative to the sequences of the bottom 25% terminators. To find tobacco-specific terminator motifs, we used STREME with the same parameters but using the top 10% *Arabidopsis* of terminators ranked by Ψ as positive and the bottom 10% of maize terminators ranked by Ψ as negative sequences. For maize-specific terminator motifs, we repeated the analysis but switched the positive and negative sequences. Meme files with all discovered motifs are available on GitHub (https://github.com/lampoona/Terminators-Plant-STARR-seq). All terminator sequences were analyzed using the universalmotif package (version 1.18.0) in R to find the position and frequency of the discovered motifs. For each sequence, the maximum motif score was identified and normalized to the minimum (set to 0) and maximum (set to 1) scores possible. Sequences with a score of at least 0.85 were considered to contain a motif match.

Computational modeling of terminator strength

In order to predict terminator strength, we first build a lasso regression model using the glmnet package (version 4.1.7) in R to predict terminator strength based on the counts of all possible, overlapping 6-mer counts. The regression model was trained on 70% of the data and tested on the remaining 30%.

For our second model, we built a convolutional neural net model using EUGENe (version 0.0.6) (Klie et al. 2022) and PyTorch ((Paszke et al. 2019); version 1.11.0) in Python (version 3.8.10). We used a “DenseNet” (Huang et al. 2017) architecture adapted from iCREPCP (Deng et al. 2023). The model takes one-hot encoded DNA as an input which is fed to a convolutional layer with 128 filters and a kernel size of 5. This layer is followed by four dense blocks consisting of 6, 12, 24, and 16 convolutional layers with 12 filters each and a kernel size of 3. In each dense block, the output of a convolutional layer is appended to its input and the combined output is used as the input for the subsequent layer. Between each dense block, the output feature map is reduced in size through convolution (using half as many filters as the input and a kernel size of 1) and average pooling (with a kernel size of 2). The output of the final dense block is fed into a fully connected layer with two outputs corresponding to the terminator

771 strength in tobacco leaves and maize protoplasts, respectively. Terminator sequences from our
772 original library that were detected in tobacco leaves and maize protoplast STARR-seq
773 experiments (*n* = 53,409) were used for model training and evaluation. Of this data, 81% were
774 used to train the model, 9% were used as a validation set during training and the remaining 10%
775 were used to test the generalizability and accuracy of the trained model. Feature attributions for
776 sequences in the test set were calculated using the DeepLIFT method (Shrikumar, Greenside,
777 and Kundaje 2017) implemented in EUGENe. These feature attributions were used as input for
778 TF-MoDISco-lite (version 2.0.6) (Shrikumar et al. 2018) to extract motifs that increase or
779 decrease terminator strength. Since we were looking for RNA motifs, we modified the TF-
780 MoDISco-lite algorithm to not consider reverse complemented seqlets for clustering, alignments,
781 or pattern generation. The code for model training and evaluation, and the trained model are
782 available on GitHub (https://github.com/lampoona/Terminators-Plant-STARR-seq).

783 *In silico* evolution of terminator sequences

784 We used the DenseNet model to iteratively improve terminator strength. We randomly
785 selected 222 sequences (111 each from *Arabidopsis* and maize) from the test set of our model
786 to ensure that the model had not seen these sequences during training. In each iteration, we
787 generated every possible point mutation for each sequence, scored them with the DenseNet
788 model, and kept the sequence variant with the highest predicted strength in tobacco leaves,
789 maize protoplasts, or both (using the sum of the activity in the individual systems) systems for
790 the next iteration. We then experimentally determined the terminator strength of the sequences
791 after three and ten rounds of evolution using Plant STARR-seq in both tobacco leaves and
792 maize protoplasts.

793 3' end sequencing

794 We used 3' end sequencing to determine the cleavage and polyadenylation site for each
795 terminator. For cDNA synthesis, we incubated 5 µL of the extracted mRNA from the second
796 Plant STARR-seq replicate in tobacco leaves with 5 µL RNase free water, 1 µL 10 mM DNTPs,
797 and 2 µL 25 mM UMI-containing oligo-dT primer for 5 min at 55°C. The solution was
798 supplemented with 4 µL 5X SuperScript IV buffer, 1 µL 100 mM DTT, 1 µL RNaseOUT, and
799 1 µL Superscript IV reverse transcriptase. The reaction was incubated for 2 min each at 4°C,
800 10°C, 20°C, 30°C, 40°C and 50°C, and finally for 15 min at 55°C. The sample was
801 supplemented with 1 µL RNase H (NEB) and incubated for 30 min at 37°C. The cDNA was
802 purified using the Zymo Clean&Concentrate-5 kit and PCR-amplified using indexed sequencing
803 primers specific to the end of the GFP construct and the adapter added using the RT primer
804 (Fig. 8a). Terminators were sequenced using an Illumina NextSeq 2000 platform with a 222-
805 nucleotide read from the 5' end of the amplicon. The paired read was used to sequence the 8-
806 nucleotide UMI. UMIs and terminator reads were linked using UMI-Tools (version 1.1.2) (Smith,
807 Heger, and Sudbery 2017). Poly-A tails of each read were removed using CutAdapt (version
808 2.5) (Kechin et al. 2017). Terminators were aligned to the designed terminator library plus 52
809 nucleotide of plasmid backbone sequence using BowTie2 (version 2.4.1) (Langmead and
810 Salzberg 2012) and reads that had a map quality of 0 or 1 were removed using Samtools
811 (version 1.9) (Li et al. 2009). Duplicate terminator-UMI pairs were removed and terminators with
812 fewer than 20 supporting reads were discarded. Bam files for each terminator were generated,
813 and cleavage sites were determined using a custom R script available on GitHub
814 (https://github.com/lampoona/Terminators-Plant-STARR-seq). Briefly, the algorithm identifies
815 local maxima in the distribution of read lengths per terminator. Cleavage probability was
816 calculated on a per terminator basis as the percentage of reads shorter than 171 nucleotides

817 (Supplementary Table 2). Major cleavage and polyadenylation sites per terminator are reported
818 in Supplementary Table 8.

819 Dual-luciferase assay

820 For the dual-luciferase assay, terminators were cloned downstream of a nanoluciferase gene
821 under control of the 35S enhancer and minimal promoter in the plasmid pDLterm
822 (https://www.addgene.org/211903/). The plasmid also harbors a luciferase gene under control of
823 the *Arabidopsis UBQ10* promoter. For the dual-luciferase assay in tobacco, two independent
824 biological replicates, with two technical replicates each, were performed. The dual-luciferase
825 reporter plasmids were introduced into *Agrobacterium tumefaciens* strain GV3101 (harboring
826 the virulence plasmid pMP90 and the helper plasmid pSoup) by electroporation and used for
827 transient transformation of tobacco leaves. Two days after the transformation, a total of 4 leaf
828 discs from the third and fourth leaf of the tobacco plants was collected using a cork borer (4 mm
829 diameter). The leaf discs were transferred to 1.5 mL tubes filled with approximately 10 glass
830 beads (1 mm diameter), snap-frozen in liquid nitrogen, and disrupted by shaking twice for 5 sec
831 in a Silamat S6 (Ivoclar) homogenizer. The leaf disc debris was resuspended in 100 µL 1X
832 Passive Lysis Buffer (Promega). The solution was cleared by centrifugation (5 min, 20,000 x g,
833 RT) and an aliquot of the supernatant was diluted 1:10 with 1X passive lysis buffer. Luciferase
834 and nanoluciferase activities were measured on a Biotek Synergy H1 plate reader using the
835 Promega Nano-Glo Dual-Luciferase Reporter Assay System according to the manufacturer's
836 instructions. Specifically, 10 µL of the diluted leaf extracts were combined with 75 µL ONE-Glo
837 EX Reagent, mixed for 3 min at 425 rpm, and incubated for 2 min before measuring luciferase
838 activity. Subsequently, 75 µL NanoDLR Stop&Glo Reagent were added to the sample. After 3
839 min mixing at 425 rpm and 12 min incubation, nanoluciferase activity was measured.
840 For the dual-luciferase assay in maize protoplasts, two independent biological replicates, with a
841 technical replicate for one of them, were performed. One million protoplasts were transformed
842 with 15 µg of the dual-luciferase reporter plasmid following the same transformation protocol as
843 used for Plant STARR-seq (see above). After incubation overnight in the dark, the transformed
844 protoplasts were washed twice with 1 mL incubation solution and lysed by adding 100 µL 1X
845 passive lysis buffer. The protoplast lysate was diluted 1:10 with 1X passive lysis buffer and used
846 to measure luciferase and nanoluciferase activities with the same protocol as used for the
847 tobacco leaf extracts. Raw values and calculated scores from assay are provided in
848 Supplementary Table 7.

849 RT-PCR and gel electrophoresis

850 To visualize terminator cleavage patterns, RNA was extracted from tobacco leaves transiently
851 transformed with dual-luciferase reporter constructs. A total of 8 leaf discs (4 mm diameter)
852 were collected two days after transformation. The fresh leaf discs were transferred to a 2 mL
853 tube containing a 5 mm stainless steel bead and 500 µL buffer RLT (QIAGEN). The leaf discs
854 were disrupted using a TissueLyser LT (QIAGEN) bead mill for 3 min at 50 Hz. Debris was
855 pelleted by centrifugation (2 mi, 20,000 x g, RT) and the supernatant was subjected to RNA
856 extraction using the QIAGEN RNease Plant Mini Kit according to the manufacturer's
857 instructions. Reverse transcription of the extracted RNA was performed in the same way as for
858 the 3' end sequencing. The resulting cDNA was PCR-amplified with primers binding to the 3'
859 end of the nanoluciferase gene and the 5' end of the reverse transcription primer. The PCR
860 products were separated by gel electrophoresis and visualized with SYBR green.
861

Data availability

All sequencing results are deposited in the NCBI Sequence Read Archive under the BioProject accession PRJNA991151.

Code availability

The code used in this study is available on GitHub (https://github.com/lampoona/Terminators-Plant-STARR-seq).

Author contributions

All authors conceived and interpreted experiments; S.G., T.J., J.T., and N.A.M performed experiments; S.G., T.J., and K.B. analyzed the data; S.G., T.J., and T.W. did the *in silico* modeling. S.G., T.J., C.Q., and S.F prepared the manuscript and figures.

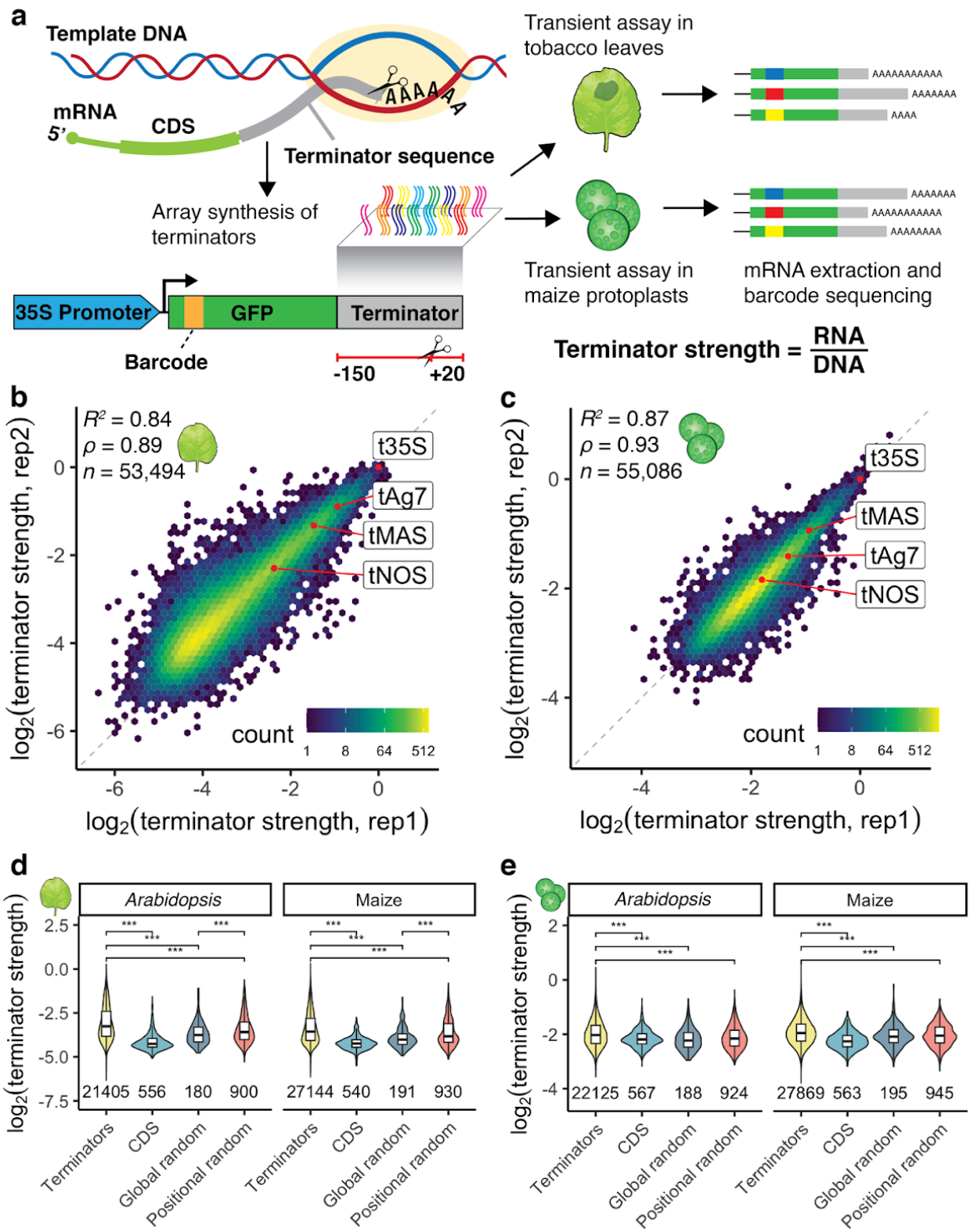

Fig. 1 | Plant STARR-seq measures terminator strength in tobacco leaves and maize protoplasts. a Terminator sequences (bases -150 to +20 relative to the cleavage and

879 polyadenylation site) were array-synthesized and cloned downstream of a barcoded GFP
880 reporter gene driven by the 35S promoter. After transient expression of the plasmid library in
881 tobacco leaves or maize protoplasts, mRNA was extracted for barcode sequencing. We define
882 terminator strength as the enrichment of barcodes in the extracted mRNA over the input DNA
883 normalized to the strength of the 35S terminator. **b, c** Hexbin plots (color represents the count of
884 points in each hexagon) of the correlation between two biological replicates of Plant STARR-seq
885 in tobacco leaves (**b**) or maize protoplasts (**c**). Commonly used terminators are highlighted in
886 red. Pearson's R^2, spearman's ρ, and number (n) of terminators are indicated. **d, e** Violin plots,
887 box plots, and significance levels of terminator strength in tobacco leaves (**d**) or maize
888 protoplasts (**e**) for plant terminators (Terminators) compared to sequences from coding regions
889 (CDS) and randomized sequences with an overall (Global random) or per-position (Positional
890 random) nucleotide frequency similar to an average *Arabidopsis* or maize terminator. Violin
891 plots represent the kernel density distribution and the box plots inside represent the median
892 (center line), upper and lower quartiles and 1.5× the interquartile range (whiskers) for all
893 corresponding terminators. Numbers at the bottom of each violin indicate the number of
894 terminators in each group. Significant differences between two samples were determined by the
895 two-sided Wilcoxon rank-sum test and are indicated: *$p \leq 0.05$, **$p \leq 0.01$, ***$p \leq 0.001$, NS, not
896 significant. Exact p values are listed in Supplementary Table 5.

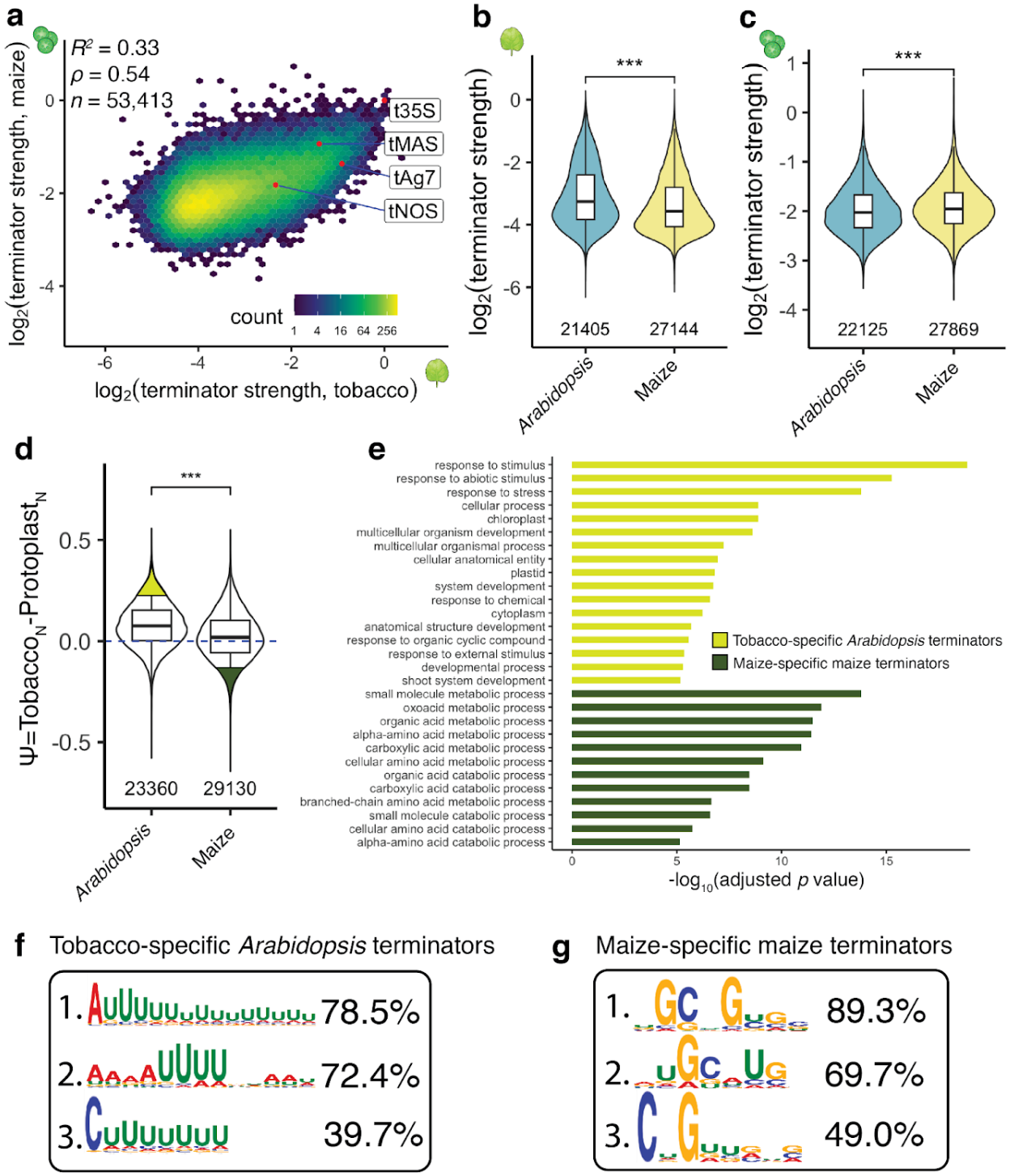

Fig. 2 | Plant terminator strength is species-specific. a Hexbin plot comparing terminator strength in tobacco leaves and maize protoplasts. **b, c** Violin plots of the strength of terminators derived from the indicated species in tobacco leaves (**b**) or maize protoplasts (**c**). **d** Violin plot of Ψ, the difference between normalized (0, weakest; 1, strongest) log2(terminator strength) in tobacco leaves (TobaccoN) and maize protoplasts (ProtoplastsN). Terminators are grouped by their species of origin. The top 10% of *Arabidopsis* terminators with highest Ψ values (tobacco-

904 specific terminators) and the top 10% of maize terminator with the lowest Ψ values (maize-
905 specific terminators) are highlighted in yellow and green, respectively. **e** GO terms enriched in
906 genes associated with the tobacco-specific Arabidopsis terminators or the maize-specific maize
907 terminators highlighted in **d**. Only GO terms with adjusted p value ≤ 0.0001 are shown. The p
908 values were determined using the gprofiler2 library in R with gSCS correction for multiple
909 testing. All enriched GO terms and exact p values are listed in Supplementary Table 6. **f, g** Top
910 three motifs enriched in tobacco-specific Arabidopsis terminators relative to maize-specific
911 maize terminators (**f**) and vice versa (**g**), with percentages denoting how many terminators per
912 group had this motif. The hexbin plot in a and the violin plots, box plots, and significance levels
913 in **b-d** are as defined in Fig. 1.
914
915
916
917
918
919
920
921
922
923
924
925
926
927

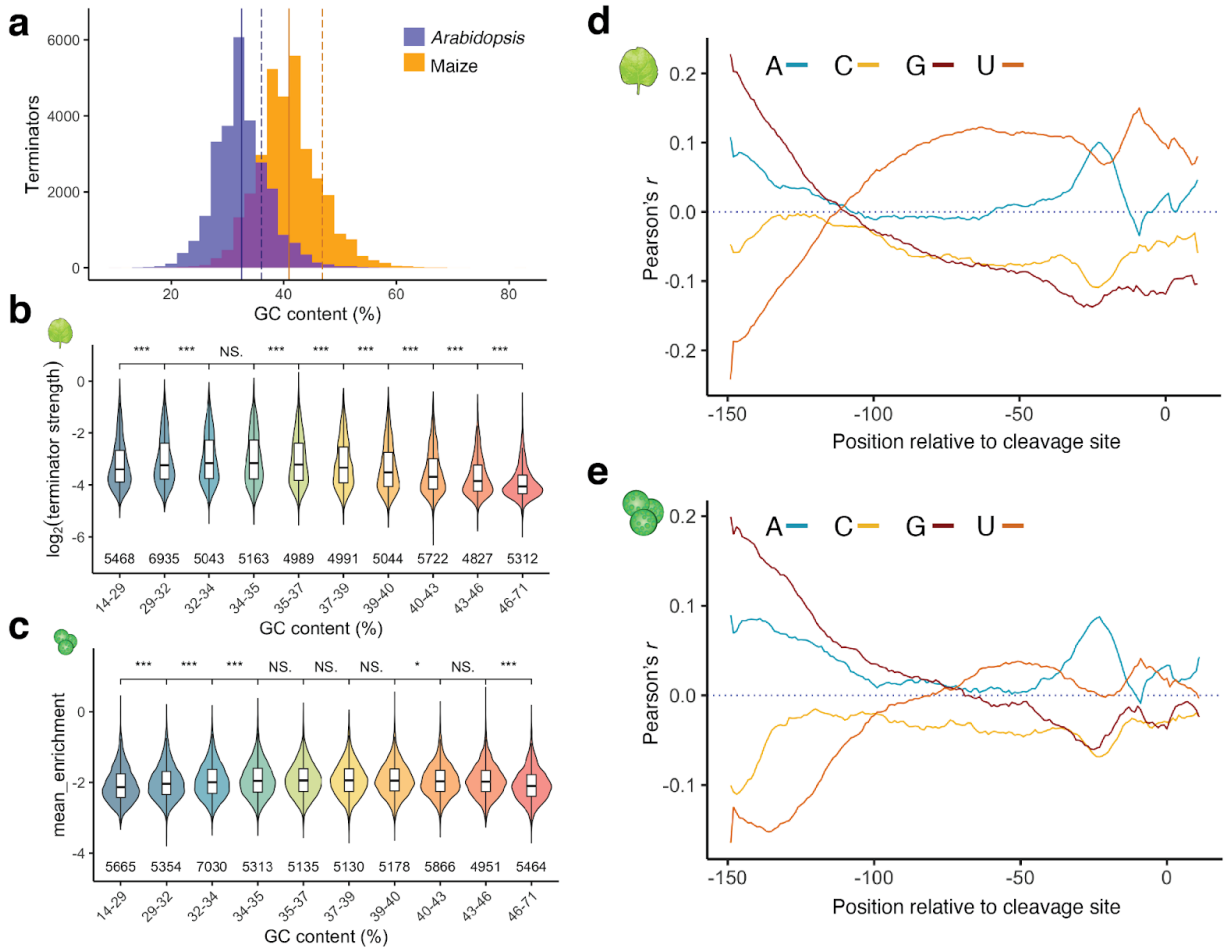

Fig. 3 | Nucleotide composition affects terminator strength in a species- and position-specific manner. a Histogram of terminator GC content. The solid line indicates the mean GC content of terminators (*Arabidopsis* = 32.53%, maize = 40.89%) and the dashed line indicates the GC content of the genome (*Arabidopsis* = 36.06%, maize = 46.86%). **b, c** Violin plots and box plots (as defined in Fig. 1) of terminator strength in tobacco leaves (**b**) or maize protoplasts (**c**). Terminators were binned by GC content to yield groups of approximately the same size. **d, e** Correlation (Pearson's *r*) between terminator strength in tobacco leaves (**d**) or maize protoplasts (**e**) and the A, C, G, or U content of a ten-base window starting at the indicated position in the plant terminators.

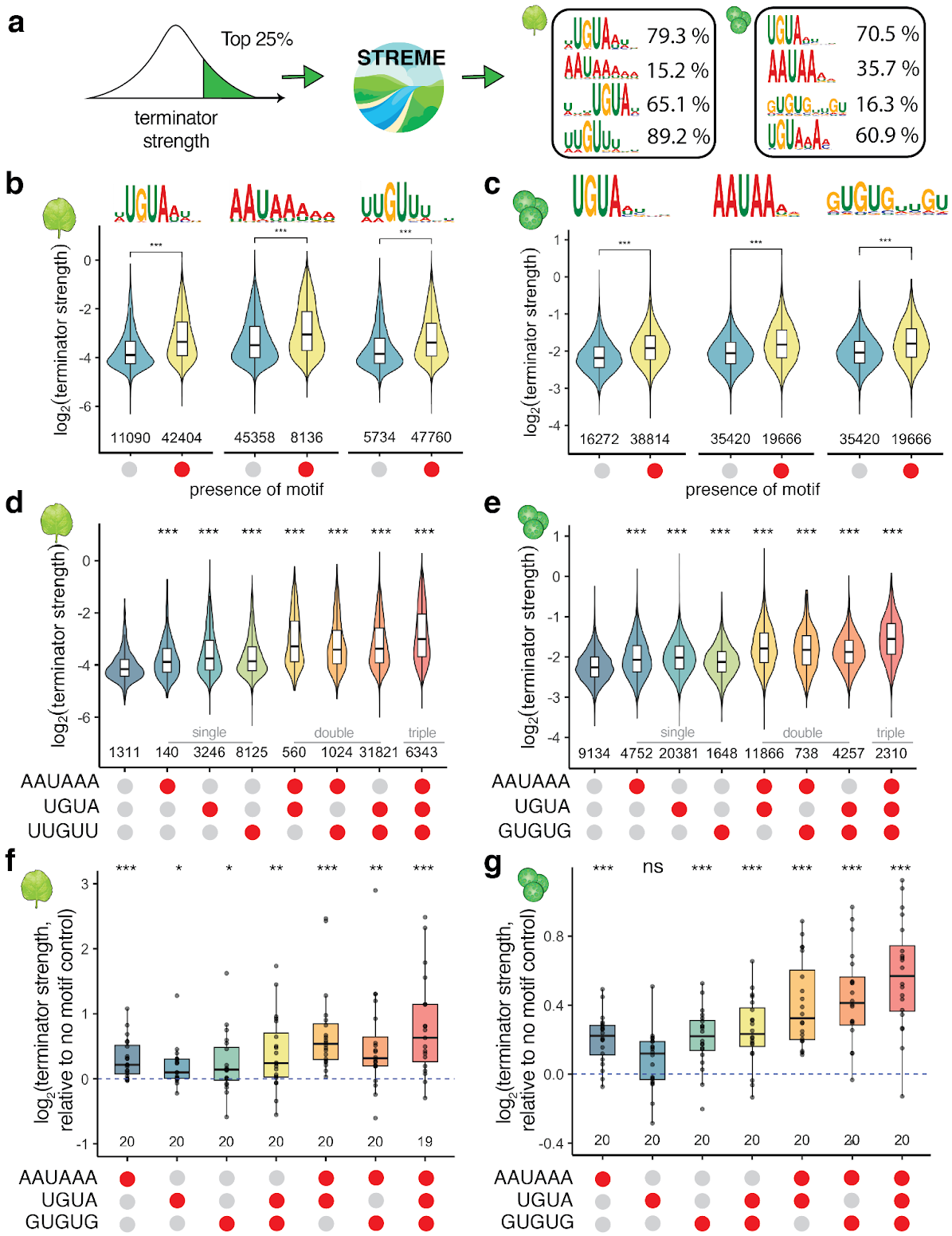

Fig. 4 | Cleavage and polyadenylation motifs increase terminator strength. a Sequence logo plots of the top four motifs enriched in the strongest terminators in tobacco leaves (left) or maize protoplasts (right). For each motif, the percentage of *Arabidopsis* and maize terminators

945 harboring it is indicated. **b**-**e** Violin plots of terminator strength in tobacco leaves (**b, d**) or maize
946 protoplasts (**c, e**) with or without AAUAAA, UGUA, or U/G-rich motifs individually (**b, c**) or in
947 combination (**d, e**). **f, g** Box plots (centre line, median; box limits, upper and lower quartiles;
948 whiskers, 1.5× interquartile range) and underlying data points for the strength of terminators
949 supplemented with the indicated motifs relative to the corresponding terminator without any
950 motif (set to 0). In **e-g,** each group is correlated with the reference group (the no motif control).
951 In **b**-**g**, red circles indicate presence of a motif and gray circles indicate its absence. Violin plots,
952 box plots, and significance levels in **b**-**g** are as defined in Fig. 1.

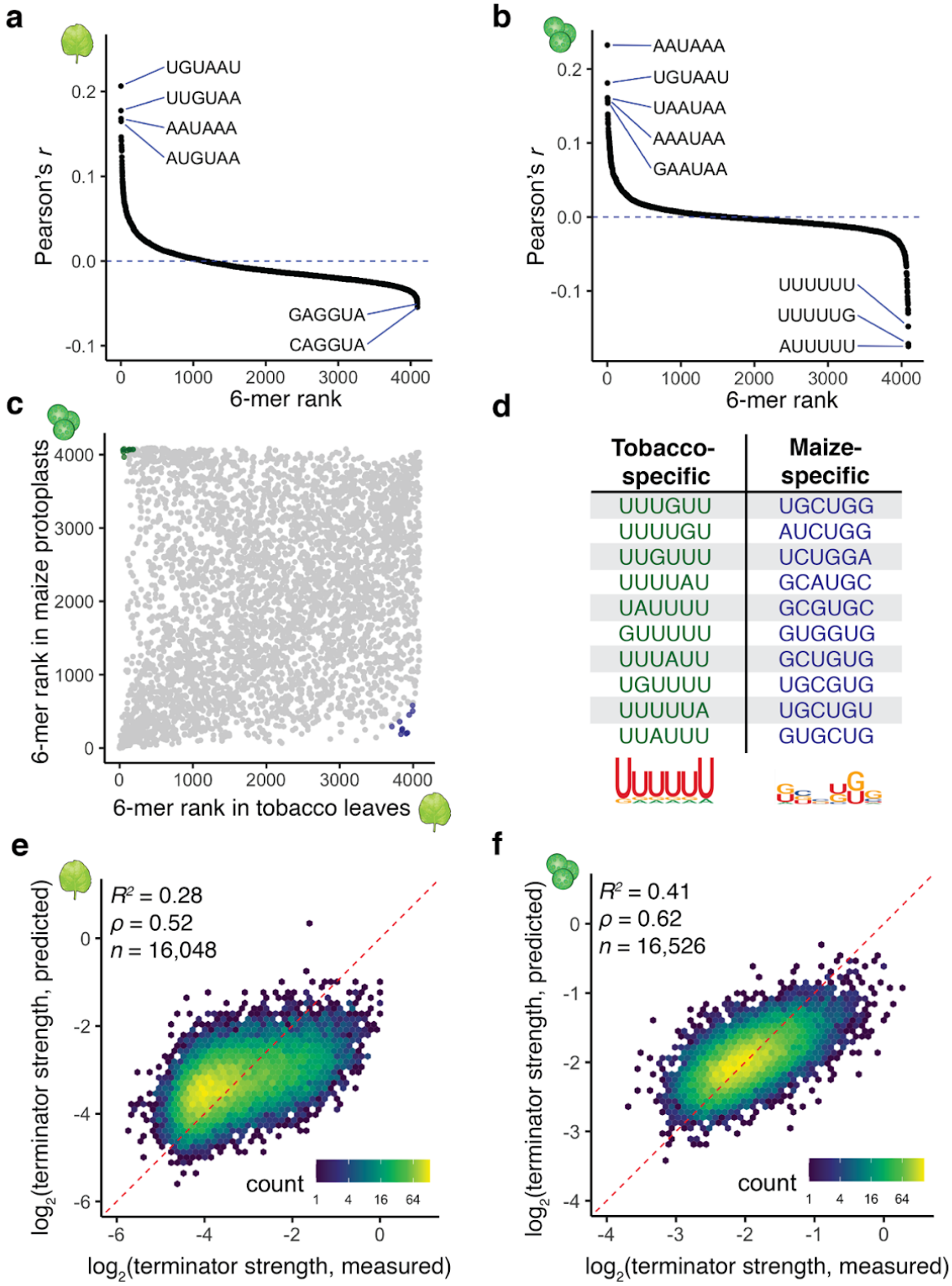

Fig. 5 | K-mers can be used for species-specific terminator strength predictions. a, b Correlation (Pearson's *r*) between terminator strength in tobacco leaves (**a**) or maize protoplasts (**b**) and how often a given 6-mer is present in the terminators. The horizontal axis displays the 6-

957 mer “rank” based on Pearson’s correlation. The sequences of the highest and lowest ranked 6-
958 mers are indicated. **c** Comparison of the 6-mer ranks in tobacco leaves and maize protoplasts.
959 6-mers highlighted in green and blue had the biggest differences in rank order between the two
960 assay systems. **d** Top 10 tobacco- or maize-specific 6-mers (highlighted in **c**) and sequence
961 logo plots generated from them. **e, f** Hexbin plot (as defined in Fig. 1) of the correlation between
962 terminator strength measured by STARR-seq in tobacco leaves (**e**) or maize protoplasts (**f**) and
963 terminator strength predictions from a lasso regression model based on 6-mer counts. Only the
964 terminators not used for model training are shown (30% of all terminators).
965

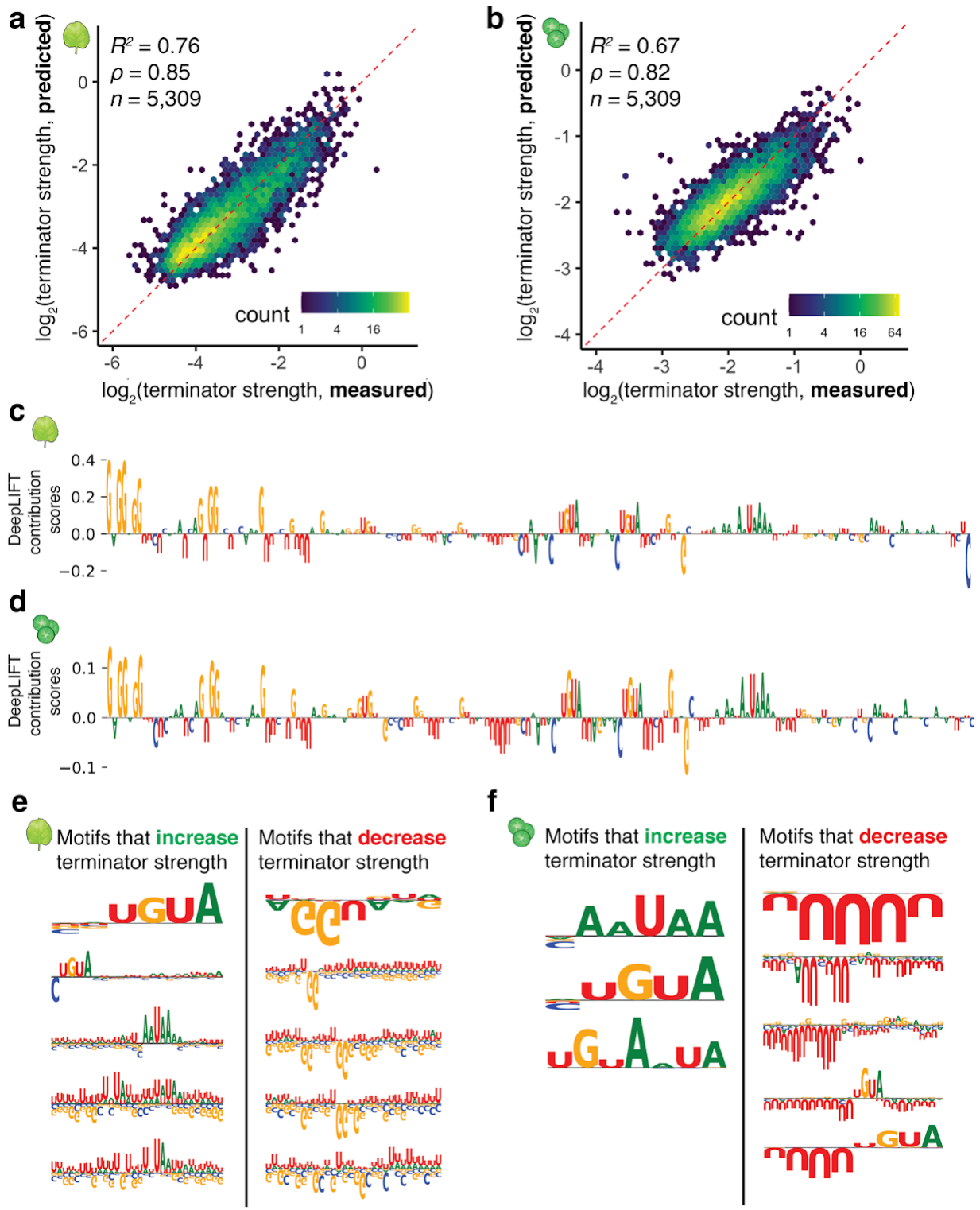

Fig. 6 | A convolutional neural network accurately predicts terminator strength. a, b Hexbin plot (as defined in Fig. 1) of the correlation between terminator strength measured by STARR-seq in tobacco leaves (**a**) or maize protoplasts (**b**) and terminator strength predictions

from a DenseNet convolutional neural network trained on terminator sequences. Only the terminators not used for model training are shown (10% of all terminators). **c, d** DeepLIFT importance scores based on our DenseNet model predictions of terminator strength in tobacco leaves (**c**) or maize protoplasts (**d**). The terminator of AT1G31180 is shown as an example. **e, f** Motifs identified by TF-MoDISco that positively or negatively contribute to the DenseNet model predictions of terminator strength in tobacco leaves (**e**) or maize protoplasts (**f**).

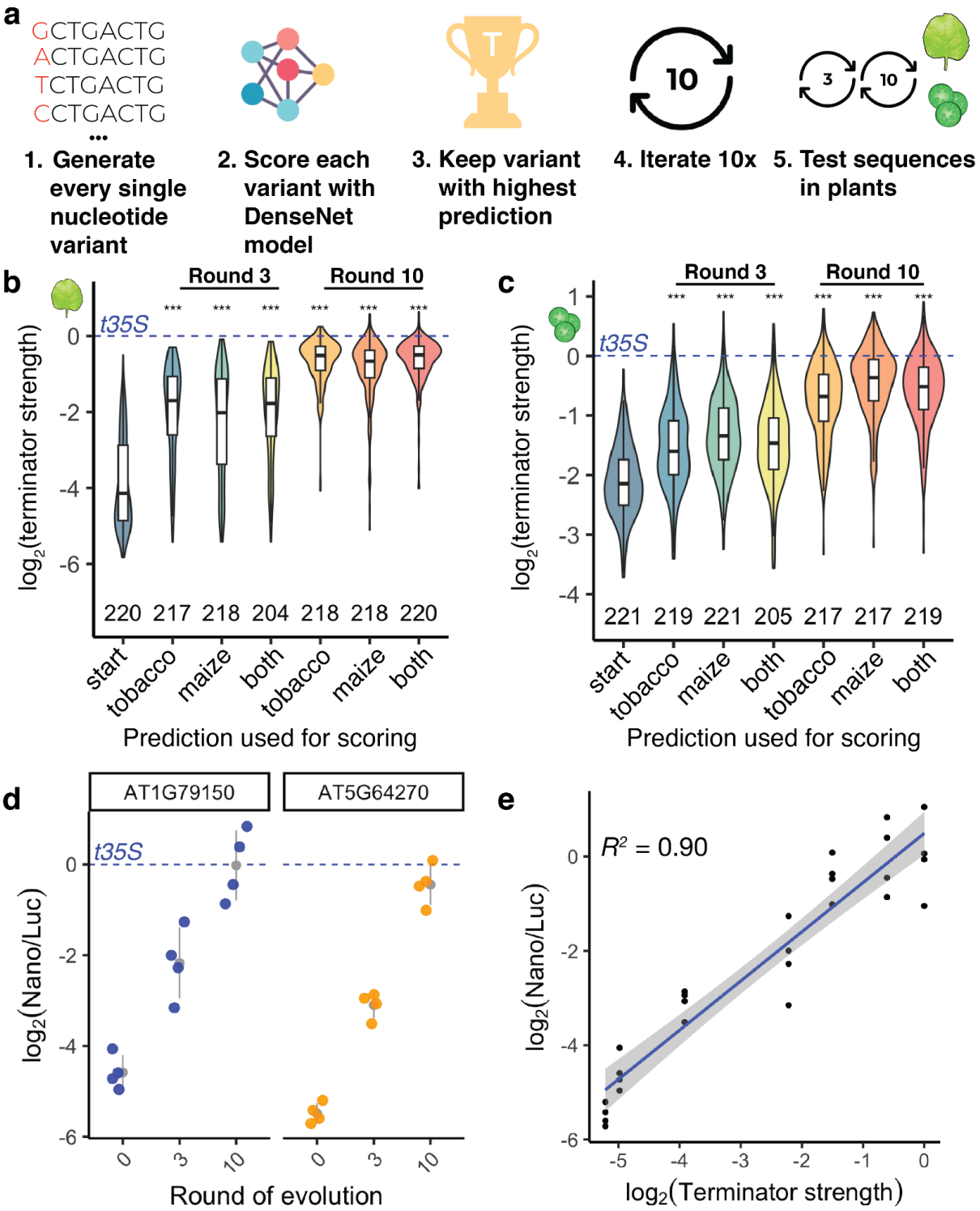

Fig. 7 | *In silico* evolution of plant terminators. a Scheme of the *in silico* evolution. **b, c** Violin plots, box plots, and significance levels (as defined in Fig. 1) of terminator strength measured in tobacco leaves (**b**) or maize protoplasts (**c**) for unmodified terminators (start) and terminators after three or ten rounds of *in silico* evolution. Groups are statistically compared to the "start" sequence. The DenseNet model prediction for tobacco leaves (tobacco) or maize protoplasts

984 (maize), or the sum of both predictions (both) was used as a score during *in silico* evolution. The
985 dashed blue line indicates the strength of the 35S terminator (*t35S*). **d** Jitter plot of the
986 nanoluciferase activity of the *in silico* evolution of AT1G79150 and AT5G64270 terminators. The
987 dashed blue line indicates the average nanoluciferase activity of the 35S terminator (*t35S*), set
988 to 0. The gray dot denotes the mean and the gray line denotes the variance. **e** Dot plot and
989 Pearson's R^2 between terminator strength and nanoluciferase activity of evolved terminators in
990 **(d)**. Raw values and calculated scores from assay are provided in Supplementary Table 7.
991
992
993
994
995

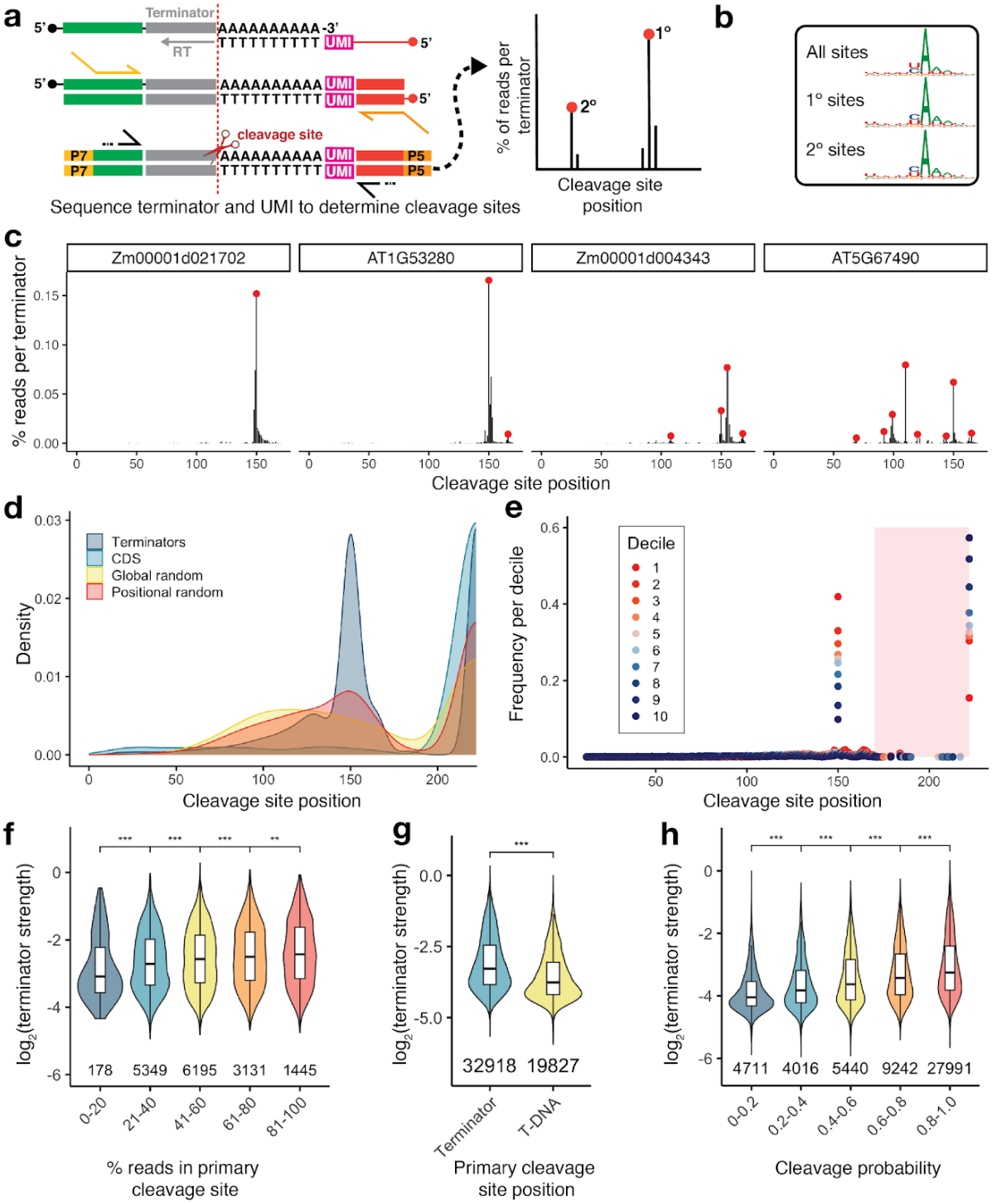

Fig. 8 | Polyadenylation and cleavage affect terminator strength. a Polyadenylation and cleavage sites for terminators in tobacco leaves were determined by 3' end sequencing. Using an oligo-dT primer with a unique molecular identifier (UMI), cDNA was generated from polyadenylated terminators. The cDNA was subjected to paired-end sequencing of the terminator and UMI. Cleavage sites were defined as local maxima in a histogram of terminator read length after trimming of the poly-A tail. **b** Sequence logo plots generated from the 10 bp window around all cleavage sites (All sites), all primary sites (1° sites), or all secondary sites (2° sites). **c** Histograms of cleavage site position for four representative terminators. Red dots

1005 denote primary and alternative cleavage sites. **d** Kernel density distribution of the primary
1006 cleavage site position for plant terminators (Terminators), sequences from coding regions
1007 (CDS), and randomized sequences with an overall (Global random) or per-position (Positional
1008 random) nucleotide frequency similar to an average *Arabidopsis* or maize terminator. **e**
1009 Histogram of the primary cleavage site position for terminators grouped into deciles based on
1010 terminator strength in tobacco leaves (decile 1 contains the strongest 10% of the terminators
1011 and decile 10 the weakest 10%). Each decile contains approximately 5,300 terminators. The
1012 shaded red area corresponds to cleavage in the T-DNA backbone (*i.e.* downstream of the
1013 terminator sequence). **f** Violin plots of terminator strength. Terminators were grouped by the
1014 percentage of reads that coincide with the primary cleavage site. **g** Violin plots of the strength of
1015 terminators with a primary cleavage site within the terminator or in the T-DNA. **h** Violin plots of
1016 terminator strength for terminators grouped by cleavage probability (percent of unique reads
1017 showing cleavage within the terminator sequence). Violin plots, box plots, and significance
1018 levels in **f**-**h** are as defined in Fig. 1. Major cleavage and polyadenylation sites per terminator
1019 are reported in Supplementary Table 8.
1020
1021

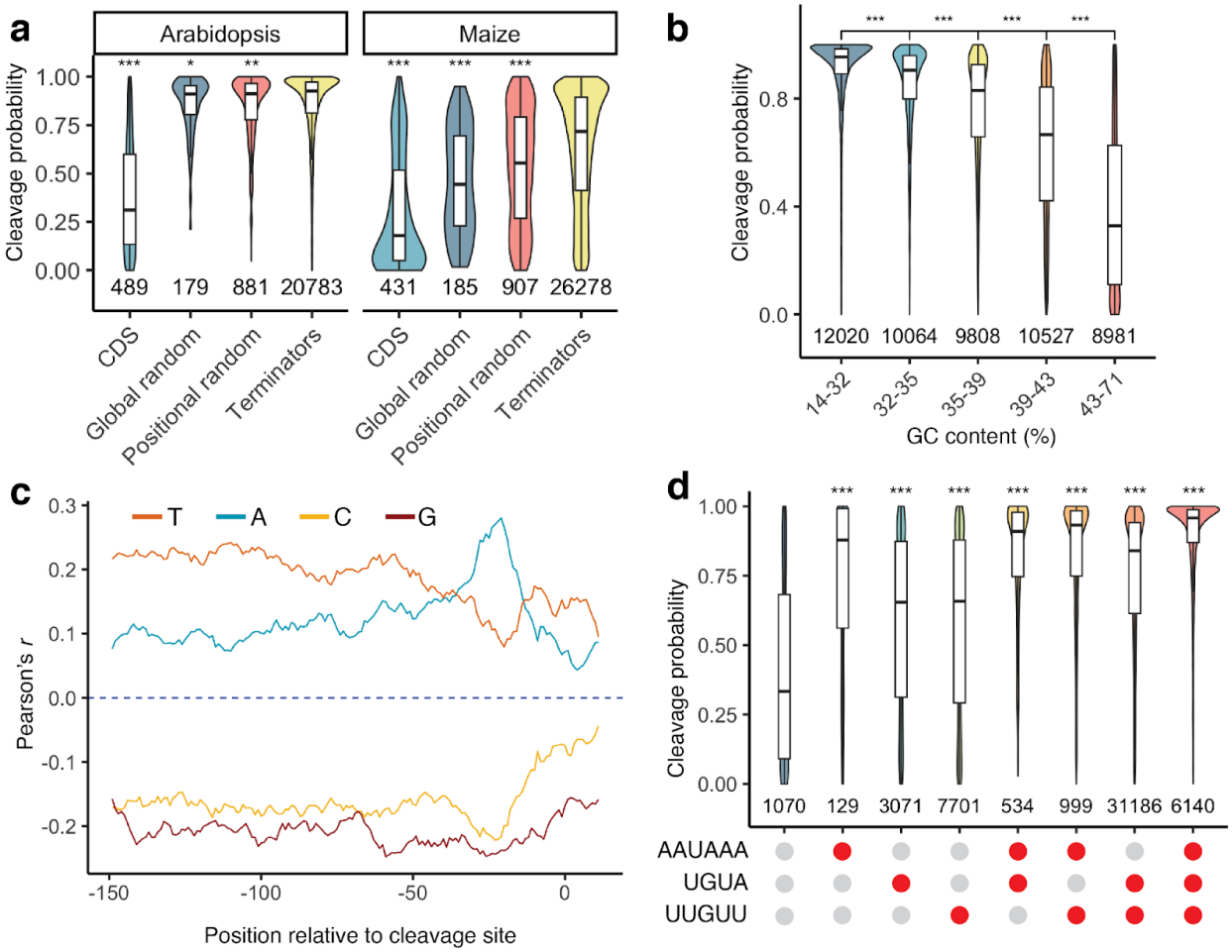

Fig. 9 | GC content and polyadenylation motifs influence cleavage probability. a Violin plots, box plots, and significance levels of cleavage probability (percent of unique reads showing cleavage within the terminator sequence) for plant terminators (Terminators) compared to sequences from coding regions (CDS) and randomized sequences with an overall (Global random) or per-position (Positional random) nucleotide frequency similar to an average *Arabidopsis* or maize terminator. Each control group is correlated to the terminator group . **b** Violin plots, box plots, and significance levels of cleavage probability. Terminators were binned by GC content to yield groups of approximately the same size. **c** Correlation (Pearson's *r*) between cleavage probability and the A, C, G, or U content of a ten-base window starting at the indicated position in the terminators. **d** Violin plots, box plots, and significance levels of cleavage probability for terminators with (red dot) or without (gray dot) the indicated motifs. Each group is correlated to the no motif control. Violin plots, box plots, and significance levels in **a**, **b**, and **d** are as defined in Fig. 1.

1045
1046 **Table 1 | Terminator polyadenylation and cleavage statistics.**

Terminator group	**Cleavage site at position 150 ± 5 bp**	**Primary cleavage site at position 150 ± 5 bp**	**Multiple cleavage sites**	**Strong secondary cleavage site (≥ 30% of reads)**	**Cleavage in T-DNA backbone only**
All terminators *n* = 54,825	33,700 (61%)	17,986 (32%)	37,301 (68%)	7,393 (13%)	9,525 (17%)
Arabidopsis terminators *n* = 22,587	15,331 (68%)	8,826 (39%)	16,827 (74%)	4,421 (20%)	1,082 (5%)
Maize terminators *n* = 27,733	16,931 (61%)	8,540 (31%)	18,008 (65%)	2,474 (9%)	6,879 (25%)
CDS *n* = 936	36 (4%)	6 (1%)	234 (25%)	17 (2%)	663 (71%)
Global random sequences *n* = 381	68 (18%)	15 (4%)	227 (60%)	53 (14%)	107 (28.1%)
Positional random terminators *n* = 1,865	773 (41)%	285 (15%)	1,250 (67%)	266 (14%)	388 (21%)

1047
1048
1049

1050

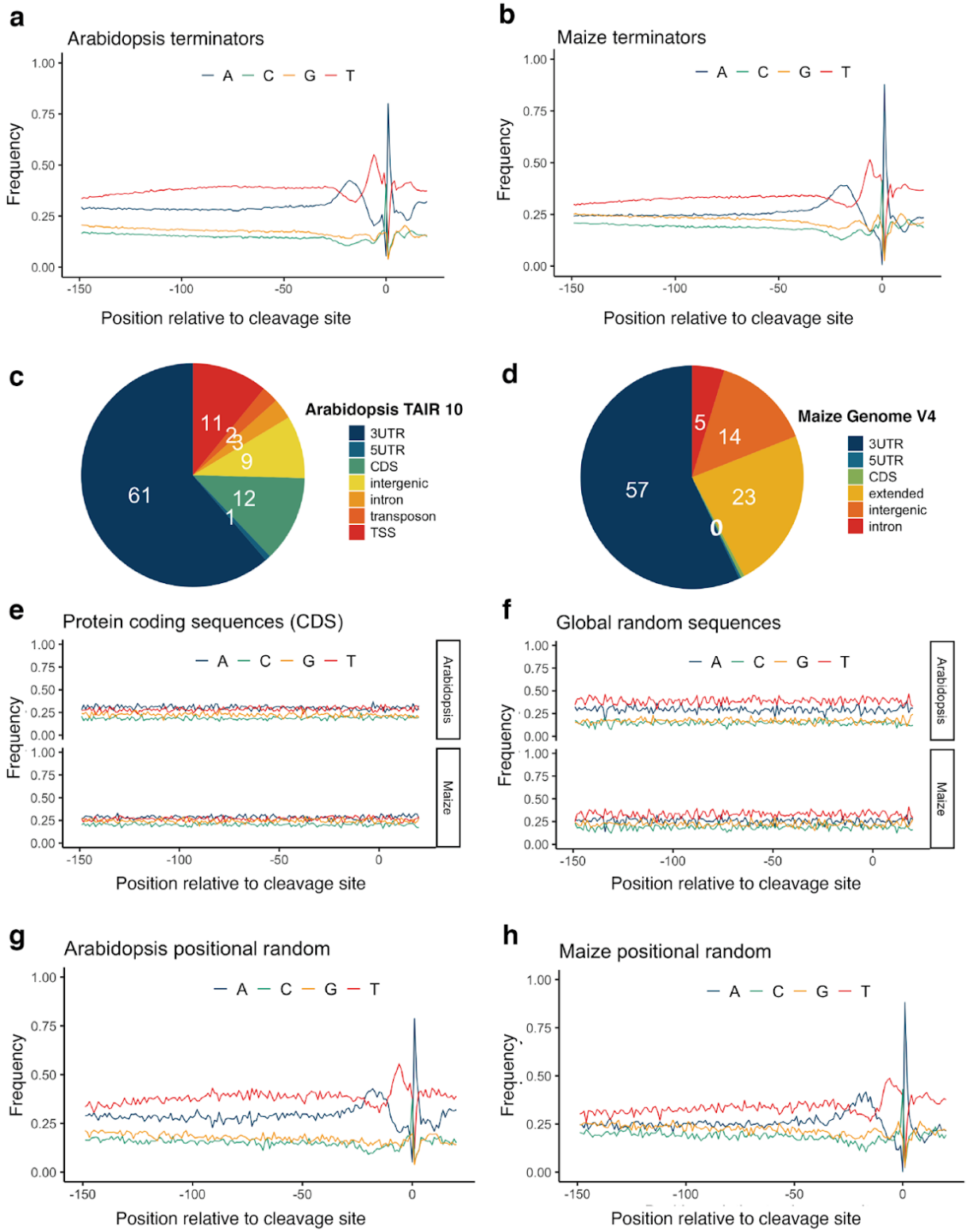

1051
1052 **Supplementary Fig. 1 | Nucleotide composition for terminators in our library. a, b** Per-
1053 position nucleotide frequencies of *Arabidopsis* (**a**) or maize (**b**) terminators. **c, d** Pie charts
1054 showing the distribution of the cleavage site location (annotated according to the *Arabidopsis*

1055 TAIR10 and the maize B73v4 genome annotations) for the terminators from *Arabidopsis* (**c**) or
1056 maize (**d**) in our library. **e** Per-position nucleotide frequencies for controls derived from coding
1057 sequences (CDS) in *Arabidopsis* or maize. **f** Per-position nucleotide frequencies of randomized
1058 sequences with an overall (Global random) nucleotide composition similar to average
1059 *Arabidopsis* or maize terminator. **g, h** Per-position nucleotide frequencies for randomized
1060 sequences with a per-position (Positional random) nucleotide composition similar to an average
1061 *Arabidopsis* (**g**) or maize (**h**) terminator.
1062
1063
1064

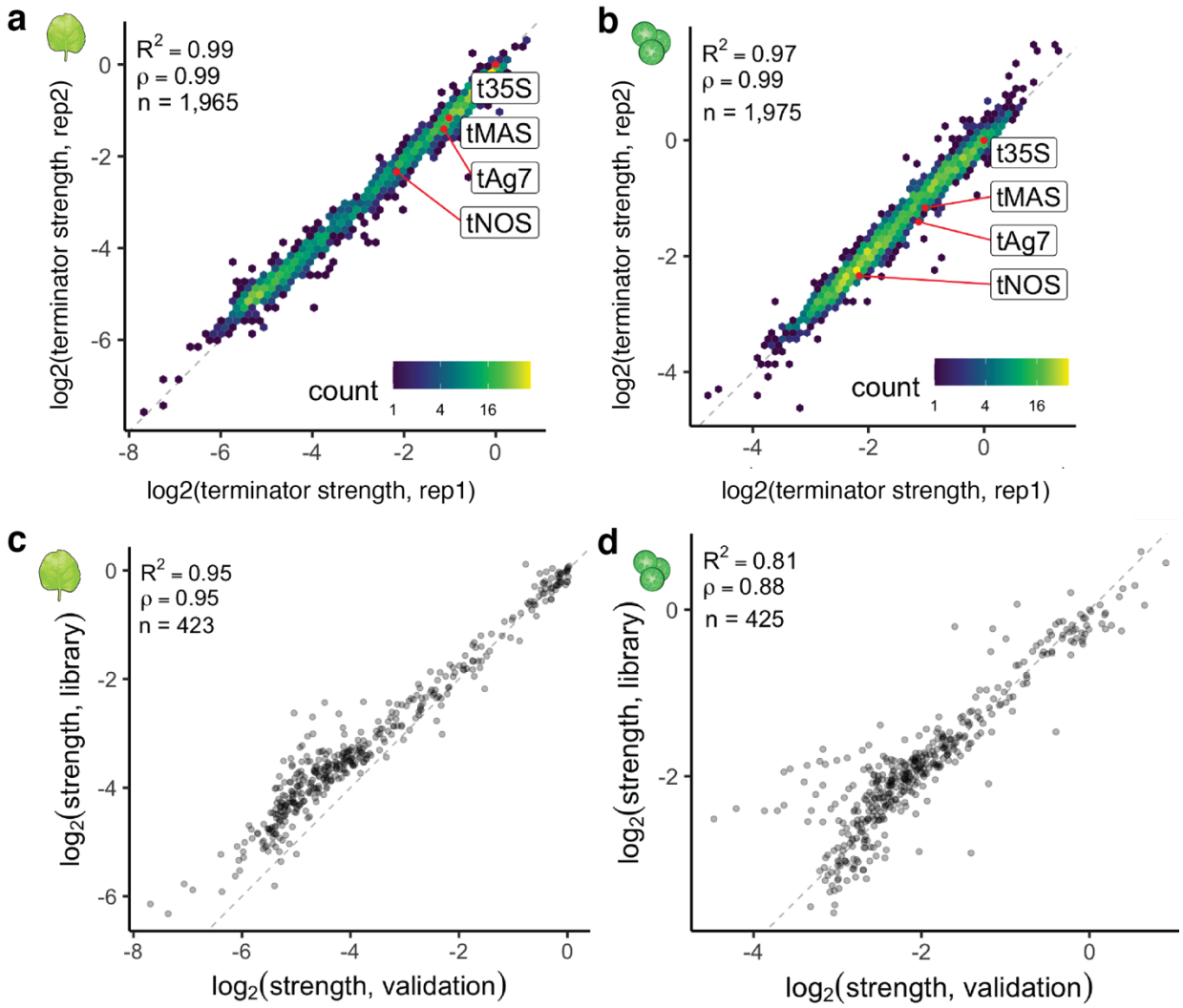

Supplementary Fig. 2 | Plant STARR-seq yields highly reproducible results across libraries. a, b Hexbin plots (as defined in Fig. 1) of the correlation between two biological replicates of Plant STARR-seq with the validation library in tobacco leaves (**a**) or maize protoplasts (**b**). Commonly used terminators are highlighted in red. **c, d** Correlation between terminator strength as measured in the large-scale library and the validation library in tobacco leaves (**c**) or maize protoplasts (**d**). Pearson's R^2, spearman's ρ, and number (n) of terminators are indicated in all plots.

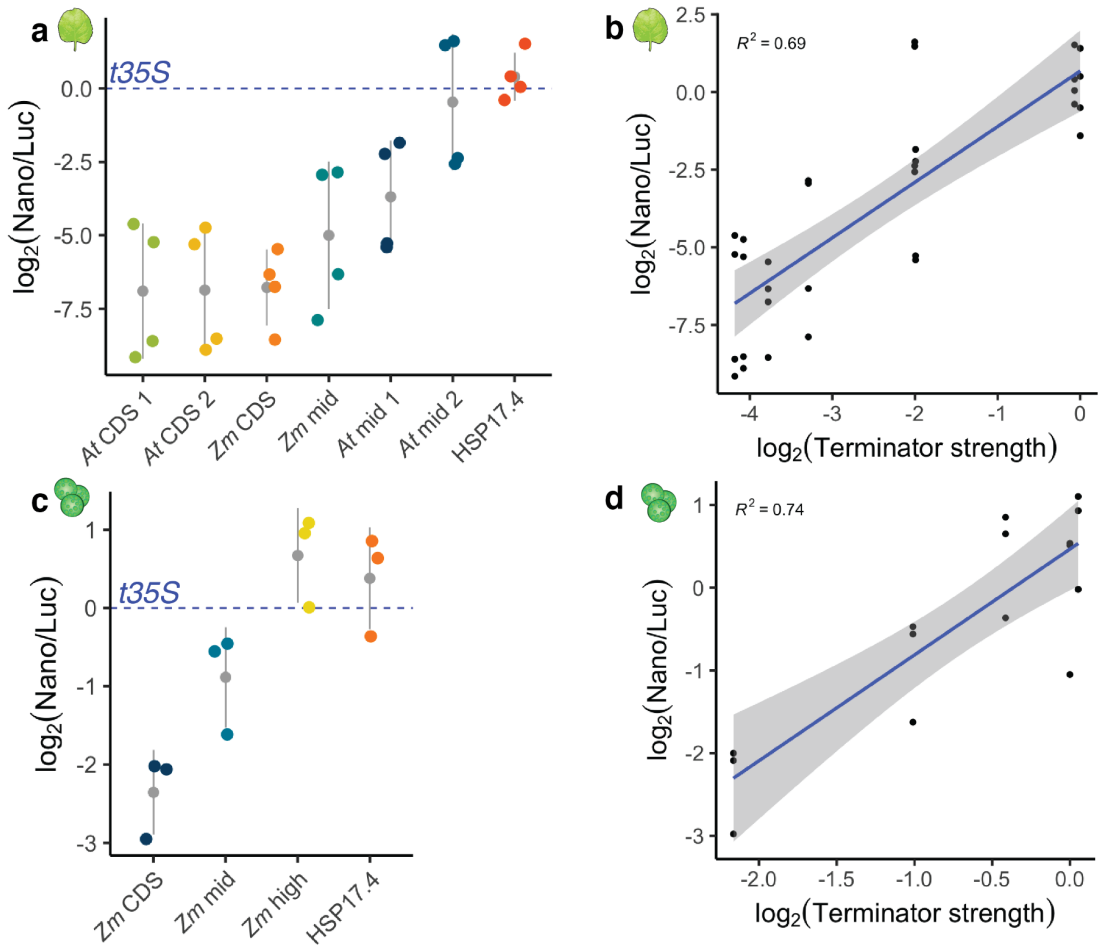

Supplementary Fig. 3 | Nanoluciferase activity (protein abundance) reflects terminator strength. Select weak (CDS), intermediate, and strong terminators are cloned immediately downstream of nanoluciferase. The nanoluciferase/luciferase ratio is normalized to a mean of the construct with the 35S terminator per experiment (35S average; log2 set to 0, dashed blue line). **a,c** Jitter plot of nanoluciferase activity for selected terminators in tobacco leaves **(a)** and maize protoplasts **(c)**. The gray dot denotes the mean and the gray line denotes the variance. **b,d** Dot plot and Pearson's R^2 between terminator strength and nanoluciferase activity of tested terminators in **(b)** tobacco leaves and **(d)** maize protoplasts. Linear regression line is shown as a blue line, and the gray band around the regression line is the 95% confidence interval. Key: {At mid 1= AT1G26300 ; AT mid 2= AT3G23110; Zm mid = Zm00001d012972_T002; At CDS 1=AT3G22360_CDS; At CDS 2= AT5G07380_CDS; Zm CDS = Zm00001d025717_T001_CDS; Zm high = Zm00001d047961_T001; HSP17.4 = AT3G46230}. Raw values and calculated scores from assay are provided in Supplementary Table 7.

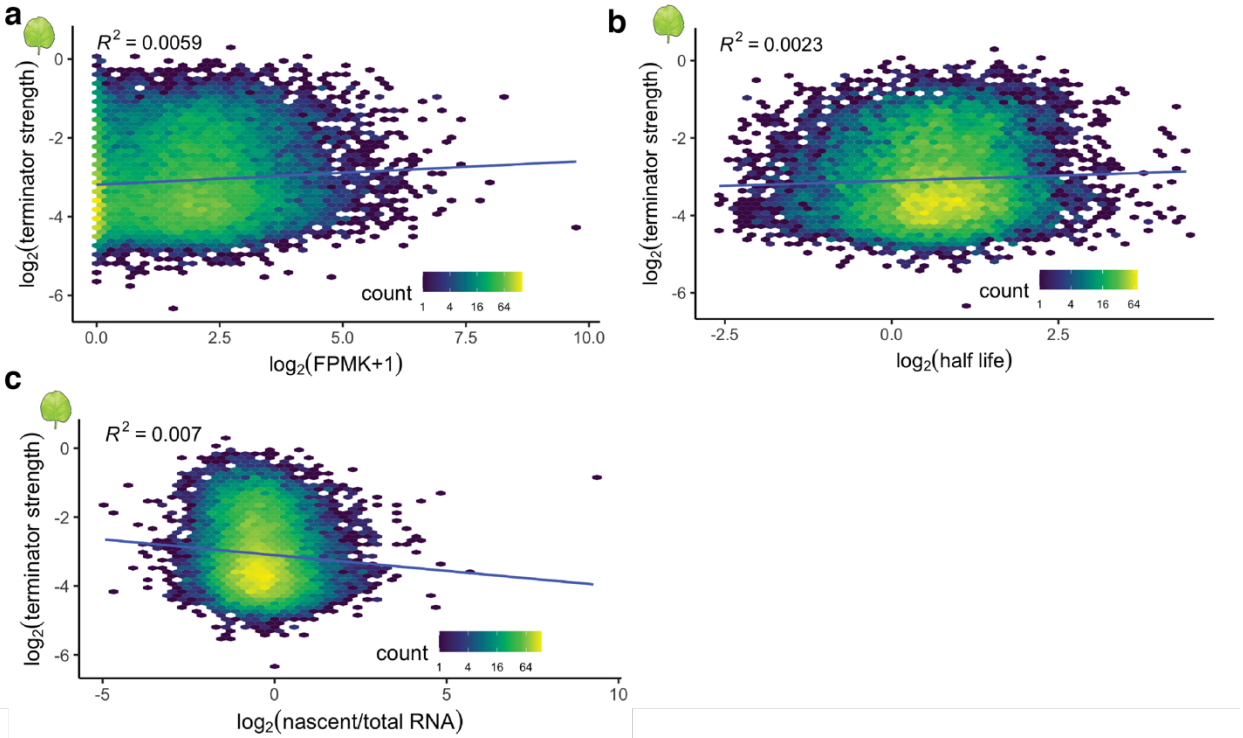

Supplementary Fig. 4 | Terminator strength is not correlated to gene expression, mRNA half-life, and nascent transcription. Hexbin plots (as defined in Fig. 1) of the correlation between the strength of *Arabidopsis* terminators and the expression (**a**), mRNA half-life (**b**), or nascent transcription (**c**) of the corresponding genes. Pearson's R^2 is indicated. See the main text for data sources.

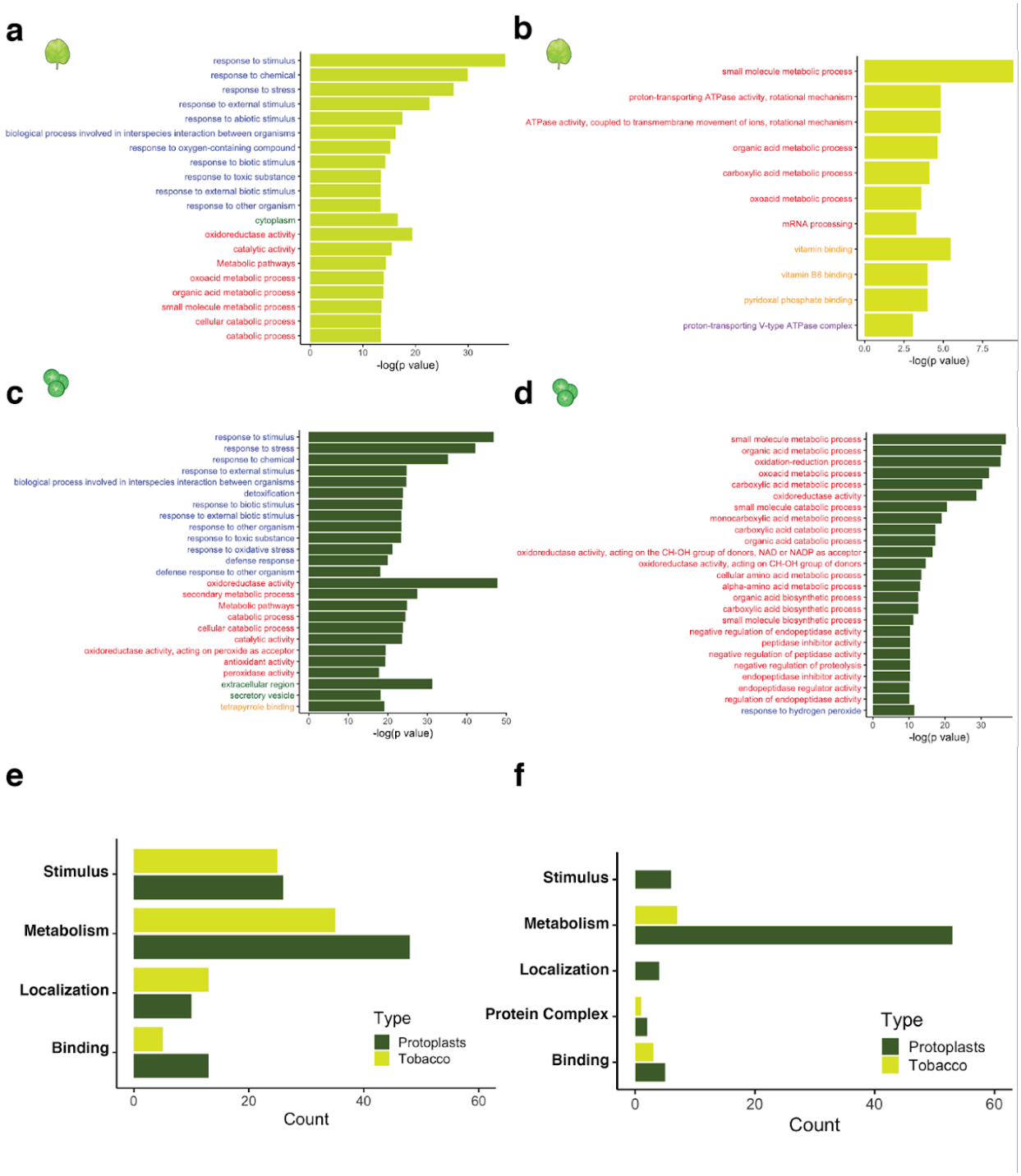

Supplementary Fig. 5 | Metabolic and stimulus-responsive genes frequently use strong terminators. a-d GO terms enriched in genes associated with the top 10% of *Arabidopsis* (**a, c**) or maize (**b, d**) terminators ranked by strength in tobacco leaves (**a, b**) or maize protoplasts (**c, d**). Only the most significant GO terms are shown. The *p* values were determined using the gprofiler2 library in R with gSCS correction for multiple testing. All enriched GO terms and exact *p* values are listed in Supplementary Table 6. **e, f** GO terms for *Arabidopsis* (**e**) or maize (**f**) terminators were collapsed into 5 major categories and counted for each assay system.

1113

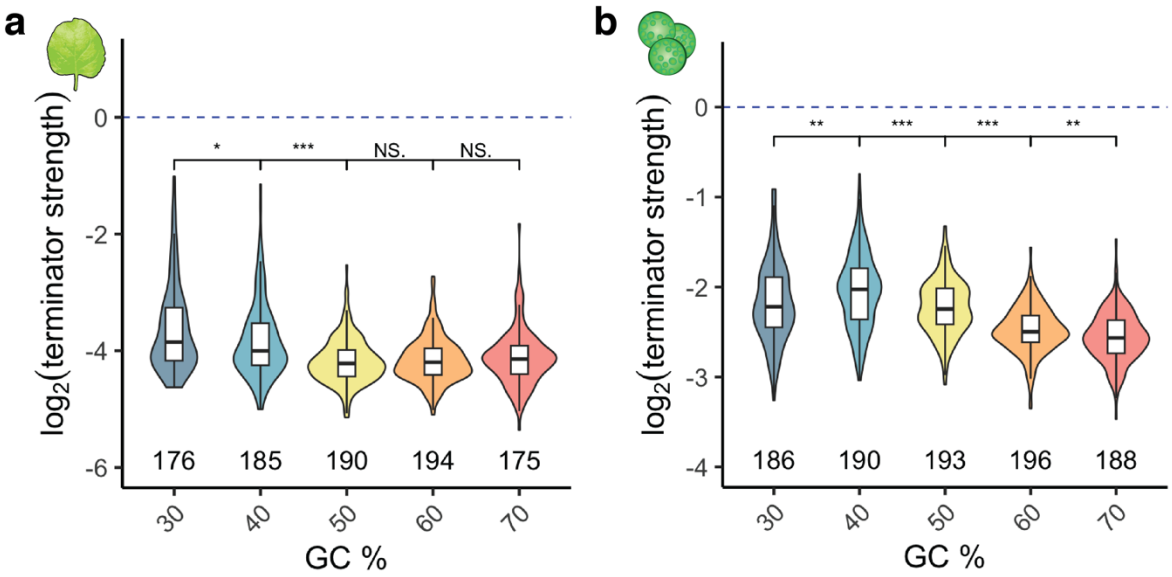

1114
1115 **Supplementary Fig. 6 | Optimal GC content for terminators is species-specific.** Violin plots,
1116 box plots, and significance levels (as defined in Fig. 1) of terminator strength in tobacco leaves
1117 (**a**) or maize protoplasts (**b**) for randomized sequences with the indicated GC content.
1118
1119

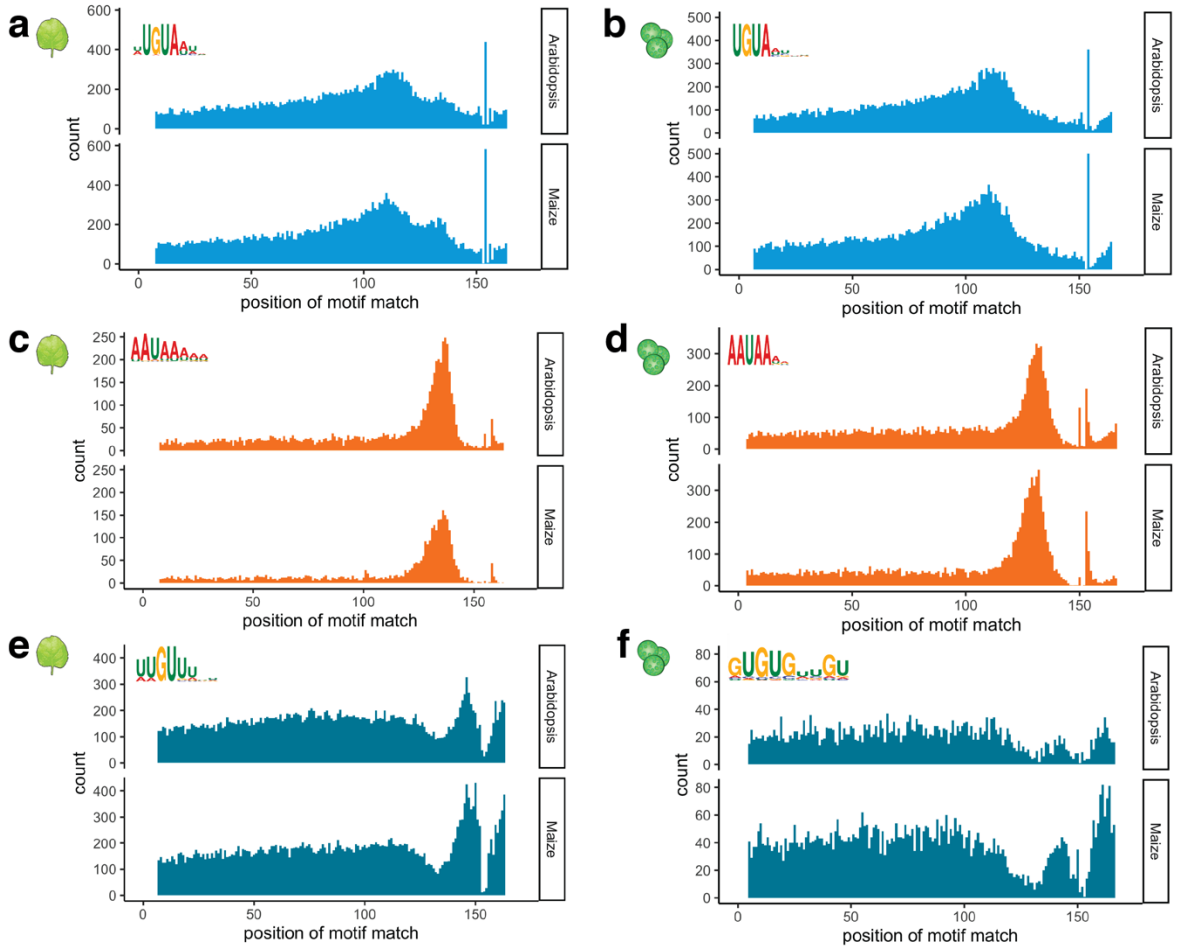

Supplementary Fig. 7 | Polyadenylation motifs show distinct localization profiles. Histograms showing the number of *Arabidopsis* and maize terminators with a UGUA motif (**a, b**), an AAUAAA motif (**c, d**), or a U/G-rich motif (**e, f**) at the indicated position. The motifs were discovered in terminators with high strength in tobacco leaves (**a, c, e**) or maize protoplasts (**b, d, f**).

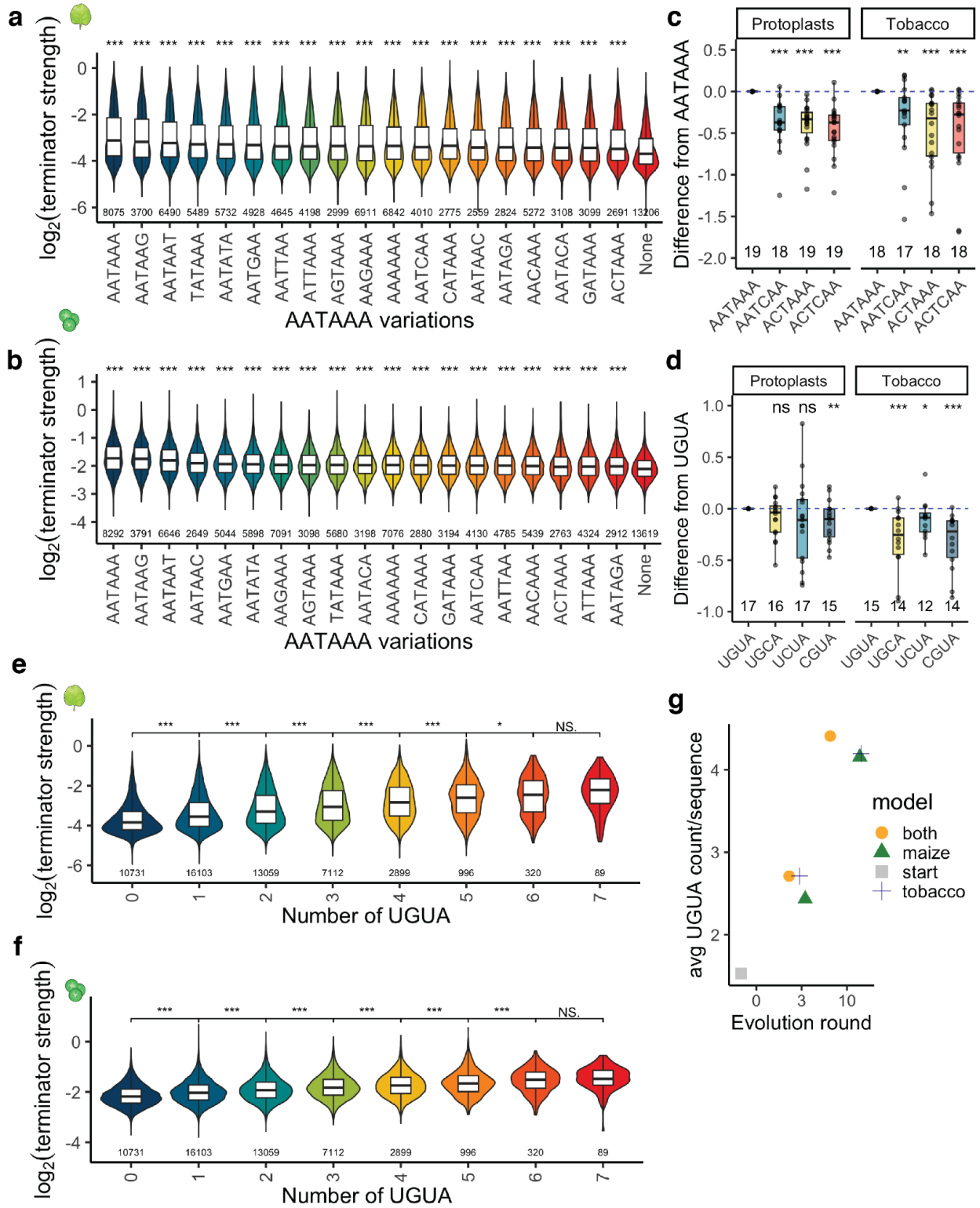

Supplementary Fig. 8 | Cleavage and polyadenylation motifs are sensitive to mutations. **a, b** Violin plots, box plots, and significance levels (as defined in Fig. 1) of terminator strength in tobacco leaves (**a**) or maize protoplasts (**b**) for terminators with the indicated variants of the AAUAAA motif. Terminators without any AAUAAA motif variant (None) are also shown. **c, d** Box

plots and significance levels (as defined in Fig. 4) of the strength of terminators with the indicated variants of the AAUAAA (**c**) or UGUA (**d**) motif relative to the strength of the corresponding wild type terminator (set to 0). **e-f** Violin plots, box plots, and significance levels (as defined in Fig. 1) of terminator strength in **(e)** tobacco leaves and **(f)** maize protoplasts of terminators with varying numbers of UGUA motifs. **g** Jitter plots of the average number of UGUA per terminator through 0, 3, and 10 rounds of *in silico* evolution.

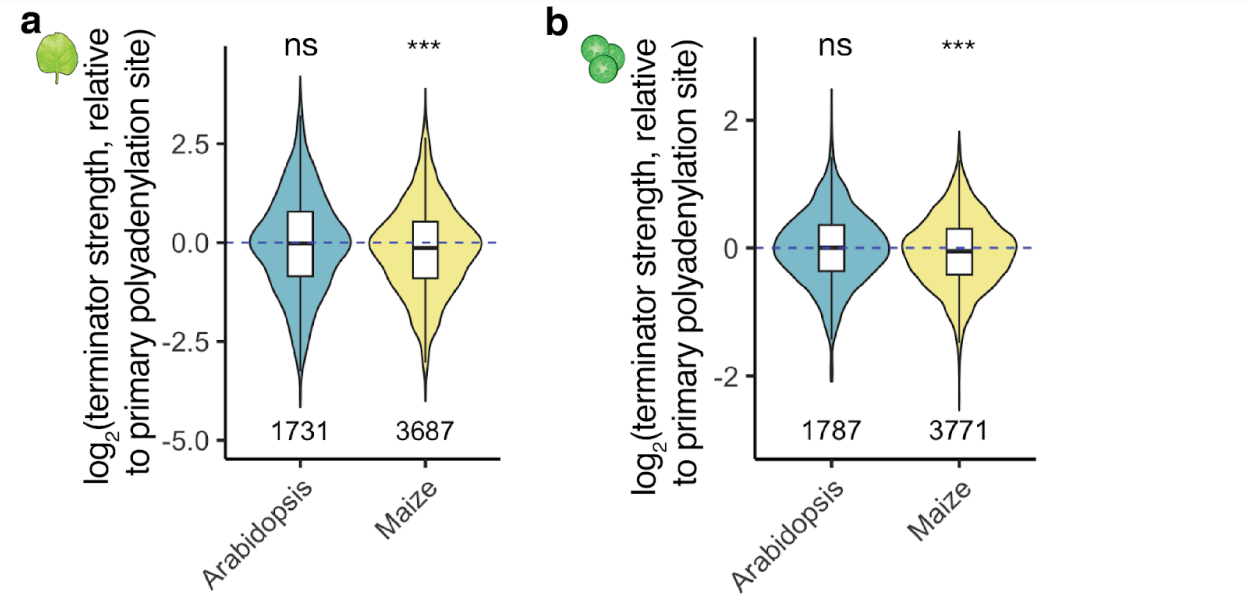

Supplementary Fig. 9 | Terminators derived from primary or secondary polyadenylation sites are indistinguishable by terminator strength. Violin plots, box plots, and significance levels (as defined in Fig. 1) of the terminator strength in tobacco leaves (**a**) or maize protoplasts (**b**) of the experimentally determined secondary polyadenylation site of *Arabidopsis* and maize genes relative to the primary polyadenylation site of the same gene (set to 0).

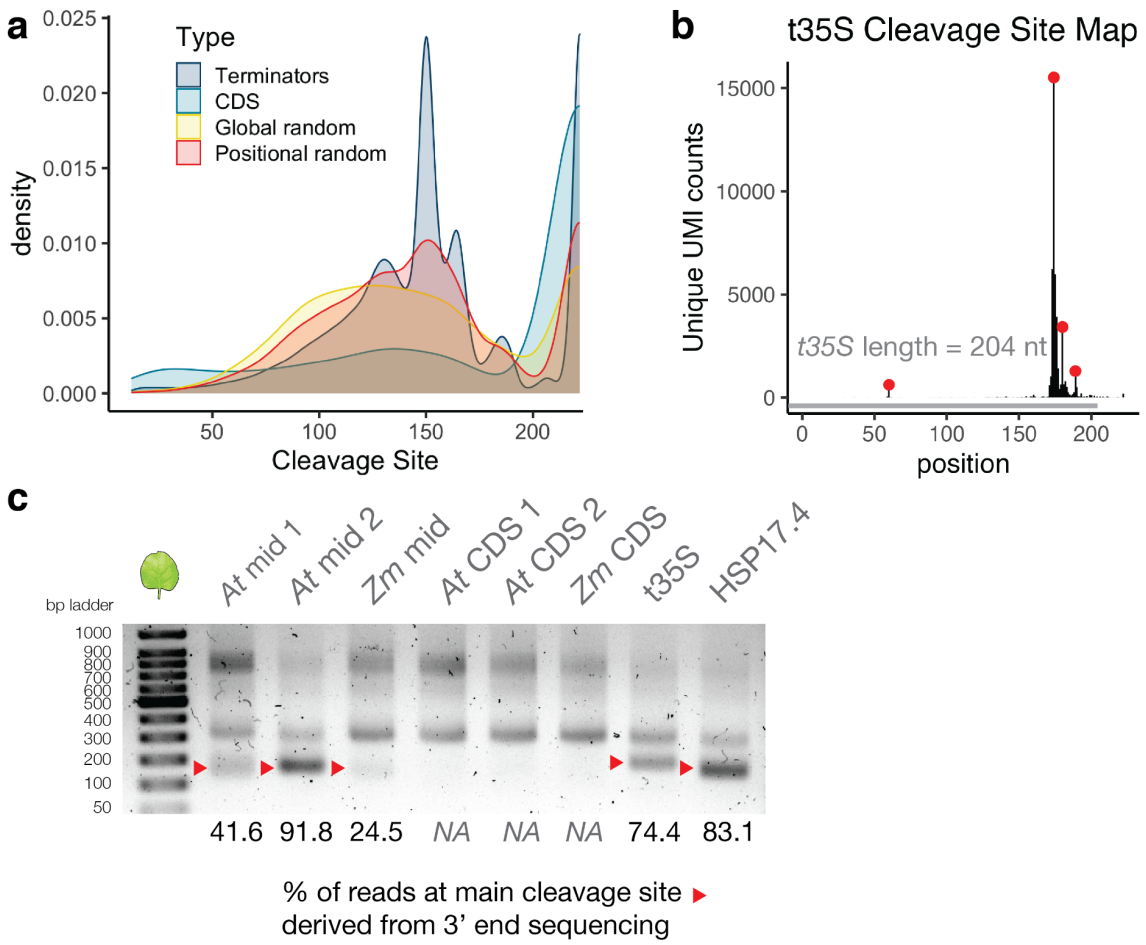

Supplementary Fig. 10 | Cleavage site positions differ between *bona fide* terminators and control sequences. a) Kernel density distribution of all cleavage site positions for plant terminators (Terminators), sequences from coding regions (CDS), and randomized sequences with an overall (Global random) or per-position (Positional random) nucleotide frequency similar to an average *Arabidopsis* or maize terminator. **b)** Cleavage site map of the CaMV 35S terminator (length=204). **c)** RNA was extracted from replicate 1 of the nanoluciferase assay (shown in Supplemental Fig 3A) and reverse transcribed using the same oligo(DT) primer for the 3' end sequencing method. cDNA was amplified and run on a 1.0% agarose gel to resolve cleavage. Red triangles denote the site of primary cleavage determined by 3'end sequencing. Key: {At mid 1= AT1G26300 ; AT mid 2= AT3G23110; Zm mid = Zm00001d012972_T002; At CDS 1=AT3G22360_CDS, At CDS 2= AT5G07380_CDS; Zm CDS = Zm00001d025717_T001_CDS, HSP17.4 = AT3G46230}

1213 **Supplementary Table 1 | Terminator library composition.**

Type	Count	Description
Arabidopsis terminators (main cleavage site)	22,204	Sequences surrounding main polyadenylation and cleavage site of *Arabidopsis* genes (-150 to +20 relative to cleavage site)
Arabidopsis terminators (secondary cleavage site)	2,325	Sequences surrounding secondary polyadenylation and cleavage site (≥30% of total reads) of *Arabidopsis* genes (-150 to +20 relative to cleavage site)
Maize terminators (main cleavage site)	25,685	Sequences surrounding main polyadenylation and cleavage site of maize genes (-150 to +20 relative to cleavage site)
Maize terminators (secondary cleavage site)	4,407	Sequences surrounding secondary polyadenylation and cleavage site (≥30% of total reads) of maize genes (-150 to +20 relative to cleavage site)
CDS	1,178	Coding sequences (170 bp) with similar overall GC content as *Arabidopsis* or maize terminators (589 from each species)
Fixed GC content	1,000	Randomized sequences (170 bp) with a GC content of: 30%, 40%, 50%, 60%, or 70% (200 each)
Global random sequences	400	Randomized sequences (170 bp) with overall nucleotide frequency similar to an average *Arabidopsis* or maize terminator (200 per species)
Positional random terminators	2,000	Randomized sequences (170 bp) with per-position nucleotide frequency similar to an average *Arabidopsis* or maize terminator (1,000 per species)
Commonly used terminators	4	35S, Ag7, NOS, and MAS terminators

1214

1215
1216
1217 **Supplementary Table 4 | Primers and DNA fragments used in this study.**

Sequence	Purpose
GTTCCACTTCTGTATAGGAGCCAATTG	linearize pPSup to build pPSt (fwd)
GGAATTCGATATCAAGCTTATCGATACCG	linearize pPSup to build pPSt (rev)
CGGTATCGATAAGCTTGATATCGAATTCCGCTGCCGTCTTCAG TGCCTGCAGGCATAGAAGACCCGTGACGAGACCACAAGGCGC GCCTAGTGGTCTCCTAAGGGAGACGGGATCCTACAGCTAGCC GTCTCGAGGTGTTCCACTTCTGTATAGGAGCCAATTG	Golden Gate cassettes for pPSt (dsDNA fragment)
GGTCGACGAAGACGGGCTG	amplify 35S promoter + Zm00001d041672 5'UTR (fwd)
GAGAGGAAGACGGTCACNNBNNGNNBNNGNNBNNBCATCGG GGAAGGCTGGG	amplify 35S promoter + Zm00001d041672 5'UTR (rev; contains barcode)
GCGCCGTCTCCTAAG<170bp_terminator>AGGTCGAGACGGTG C	terminator oligo pool
GCGCCGTCTCCTAAG	amplify terminator oligo pool (fwd)
GCACCGTCTCGACCT	amplify terminator oligo pool (rev)
CAGGTCGACGGTCTCCGTGAGCAAGGGCGAGGAG	amplify GFP (fwd)
TCCTCTAGAGGTCTCGCTTACTTGTACAGCTCGTCCATGCC	amplify GFP (rev)
AGTTCAGCCACATGGTCCTGCTGGAGTTC	delete central portion of GFP (fwd)
GGACCATGTGGCTGAACTTGTGGCCGTTTA	delete central portion of GFP (rev)
GGACGACGTCGTCTCCTAAGCTCTAGCTAGAGTCGATCGACA AGCTCGAGTTTCTCCATAATAATGTGTGAGTAGTTCCCAGATA AGGGAATTAGGGTTCCTATAGGGTTTCGCTCATGTGTTGAGCA TATAAGAAACCCTTAGTATGTATTTGTATTTGTAAAATACTTCTA TCAATAAAATTTCTAATTCCTAAAACCAAAATCCAGTACTAAAAT CCAGATAGGTCGAGACGACGTCGTAC	template 35S terminator
GGACGACGTCGTCTCCTAAGCTCTAGCTAGAGTCGATCG	amplify 35S terminator (fwd)
GTACGACGTCGTCTCGACCTATCTGGATTTTAGTACTGGATTT TG	amplify 35S terminator (rev)
GGACGACGTCGTCTCCTAAGGATCGTTCAAACATTTGGC	amplify NOS terminator (fwd)
GTACGACGTCGTCTCGACCTGATCTAGTAACATAGATGACACC	amplify NOS terminator (rev)
GGACGACGTCGTCTCCTAAGCTTGGACTCCCATGTTGGCAAA GGCAACCAAACAAACAATGAATGATCCGCTCCTGCATATGGG GCGGTTTGAGTATTTCAACTGCCATTTGGGCTGAATTGTAGAC ATGCTCCTGTCAGAAATTCCGTGATCTTACTCAATATTCAGTAA TCTCGGCCAATATCCTAAATGTGCGTGGCTTTATCTGTCTTTGT ATTGTTTCATCAATTCATGTAACGTTTGCTTTTCTTATGAATTTT CAAATAAATTATCAGGTCGAGACGACGTCGTAC	template MAS terminator
GGACGACGTCGTCTCCTAAGCTTGGACTCCCATGTTG	amplify MAS terminator (fwd)

GTACGACGTCGTCTCGACCTGATAATTTATTTGAAAATTCATAAGAA	amplify MAS terminator (rev)
GGACGACGTCGTCTCCTAAGGCTAGCTATATCATCAATTTATGTATTACACATAATATCGCACTCAGTCTTTCATCTACGGCAATGTACCAGCTGATATAATCAGTTATTGAAATATTTCTGAATTTAAACTTGCATCAATAAATTTATGTTTTTGCTTGGACTATAATACCTGACTTGTTATTTTATCAATAAATATTTAAACTATATTTCTTTCAAGATGGGAATTAGGTCGAGACGACGTCGTAC	template Ag7 terminator
GGACGACGTCGTCTCCTAAGGCTAGCTATATCATCAATTTATG	amplify Ag7 terminator (fwd)
GTACGACGTCGTCTCGACCTAATTCCCATCTTGAAAGAAATATAGT	amplify Ag7 terminator (rev)
GAACTTGTGGCCGTTTACG	reverse transcription for barcode sequencing
AATGATACGGCGACCACCGAGATCTACAC<8bp_index2>CCTCGGCCTCCCTGTCC	amplify barcode for NGS (fwd)
CAAGCAGAAGACGGCATACGAGAT<8bp_index1>CACCCCGGTGAACAGCTCC	amplify barcode for NGS (rev)
CCTCGGCCTCCCTGTCCCCAGCCTTCCCCGATG	NGS read 1 primer for barcode sequencing
CACCCCGGTGAACAGCTCCTCGCCCTTGCTCAC	NGS read 2 primer for barcode sequencing
GTGAGCAAGGGCGAGGAGCTGTTCACCGGGGTG	NGS index 1 primer for barcode sequencing
CATCGGGGAAGGCTGGGGACAGGGAGGCCGAGG	NGS index 2 primer for barcode sequencing
ACGACGCTCTTCCGATCTNNNNNNNNTTTTTTTTTTTTTTTTTTTTTTTTTTTTVN	reverse transcription primer for 3’ end sequencing
AATGATACGGCGACCACCGAGATCTACAC<8bp_index2>GGATCACTCACGGCATGGAC	amplify terminator 3’ end (fwd)
CAAGCAGAAGACGGCATACGAGAT<8bp_index1>ACACTCTTTCCCTACACGACGCTCTTCCGATCT	amplify terminator 3’ end (rev)
GGATCACTCACGGCATGGACGAGCTGTACAAGTAAG	NGS read 1 primer for 3’ end sequencing
Illumina TruSeq read 1 primer (ACACTCTTTCCCTACACGACGCTCTTCCGATCT)	NGS read 2 primer for 3’ end sequencing
Illumina TruSeq index 2 primer (AGATCGGAAGAGCGTCGTGTAGGGAAAGAGTGT)	NGS index 1 primer for 3’ end sequencing
CTTACTTGTACAGCTCGTCCATGCCGTGAGTGATCC	NGS index 2 primer for 3’ end sequencing
AATGATACGGCGACCACCGAGATCTACAC<8bp_index2>CCTCGGCCTCCCTGTCC	amplify terminator library for subassembly (fwd)
CAAGCAGAAGACGGCATACGAGATGCAACCAAGATGCATGTTGTCATCATTGGCTCC	amplify terminator library for subassembly (rev)
GGATCACTCACGGCATGGACGAGCTGTACAAGTAAG	NGS read 1 primer for subassembly sequencing
GATGCATGTTGTCATCATTGGCTCCTATACAGAAGTGGAACACCT	NGS read 2 primer for subassembly sequencing

CCTCGGCCTCCCTGTCCCCAGCCTTCCCCGATG	NGS index 1 primer for subassembly sequencing
CACCCCGGTGAACAGCTCCTCGCCCTTGCTCAC	NGS index 2 primer for subassembly sequencing
GAGTAACCATCAACGGAGTGACC	Amplify nanoluciferase terminators for gel
ACGACGCTCTTCCGATCT	Amplify nanoluciferase terminators for gel

1218

References

Allen, Edwards, and Miya D. Howell. 2010. “miRNAs in the Biogenesis of Trans-Acting siRNAs in Higher Plants.” *Seminars in Cell & Developmental Biology* 21 (8): 798–804.

Andreou, Andreas I., Jessica Nirkko, Marisol Ochoa-Villarreal, and Naomi Nakayama. 2021. “Mobius Assembly for Plant Systems Highlights Promoter-Terminator Interaction in Gene Regulation.” *bioRxiv*. https://doi.org/10.1101/2021.03.31.437819.

Baeg, Kyungmin, Hiro-Oki Iwakawa, and Yukihide Tomari. 2017. “The poly(A) Tail Blocks RDR6 from Converting Self mRNAs into Substrates for Gene Silencing.” *Nature Plants* 3 (March): 17036.

Bailey, Timothy L. 2021. “STREME: Accurate and Versatile Sequence Motif Discovery.” *Bioinformatics* 37 (18): 2834–40.

Bell, Stephen A., and Arthur G. Hunt. 2010. “The Arabidopsis Ortholog of the 77 kDa Subunit of the Cleavage Stimulatory Factor (AtCstF-77) Involved in mRNA Polyadenylation Is an RNA-Binding Protein.” *FEBS Letters* 584 (8): 1449–54.

Bernardes, Willian Souza, and Marcelo Menossi. 2020. “Plant 3’ Regulatory Regions From mRNA-Encoding Genes and Their Uses to Modulate Expression.” *Frontiers in Plant Science*. https://doi.org/10.3389/fpls.2020.01252.

Beyer, K., T. Dandekar, and W. Keller. 1997. “RNA Ligands Selected by Cleavage Stimulation Factor Contain Distinct Sequence Motifs That Function as Downstream Elements in 3’-End Processing of Pre-mRNA.” *The Journal of Biological Chemistry* 272 (42): 26769–79.

Birse, C. E., L. Minvielle-Sebastia, B. A. Lee, W. Keller, and N. J. Proudfoot. 1998. “Coupling Termination of Transcription to Messenger RNA Maturation in Yeast.” *Science* 280 (5361): 298–301.

Brooks, Emily G., Estefania Elorriaga, Yang Liu, James R. Duduit, Guoliang Yuan, Chung-Jui Tsai, Gerald A. Tuskan, Thomas G. Ranney, Xiaohan Yang, and Wusheng Liu. 2023. “Plant Promoters and Terminators for High-Precision Bioengineering.” *Biodesign Research* 5 (July): 0013.

Chang, Jae-Woong, Wei Zhang, Hsin-Sung Yeh, Ebbing P. de Jong, Semo Jun, Kwan-Hyun Kim, Sun S. Bae, et al. 2015. “mRNA 3′-UTR Shortening Is a Molecular Signature of mTORC1 Activation.” *Nature Communications*. https://doi.org/10.1038/ncomms8218.

Connelly, S., and J. L. Manley. 1988. “A Functional mRNA Polyadenylation Signal Is Required for Transcription Termination by RNA Polymerase II.” *Genes & Development* 2 (4): 440–52.

Cuperus, Josh T., Benjamin Groves, Anna Kuchina, Alexander B. Rosenberg, Nebojsa Jojic, Stanley Fields, and Georg Seelig. 2017. “Deep Learning of the Regulatory Grammar of Yeast 5’ Untranslated Regions from 500,000 Random Sequences.” *Genome Research* 27 (12): 2015–24.

Dadami, Elena, Athanasios Dalakouras, Michele Zwiebel, Gabi Krczal, and Michael Wassenegger. 2014. “An Endogene-Resembling Transgene Is Resistant to DNA Methylation and Systemic Silencing.” *RNA Biology* 11 (7): 934–41.

Deng, Kaixuan, Qizhe Zhang, Yuxin Hong, Jianbing Yan, and Xuehai Hu. 2023. “iCREPCP: A Deep Learning-Based Web Server for Identifying Base-Resolution Cis-Regulatory Elements within Plant Core Promoters.” *Plant Communications* 4 (1): 100455.

Department of Economic and Social Affairs. 2022. *World Economic Situation and Prospects 2022*. United Nations.

Diamos, Andrew G., and Hugh S. Mason. 2018. “Chimeric 3’ Flanking Regions Strongly Enhance Gene Expression in Plants.” *Plant Biotechnology Journal* 16 (12): 1971–82.

Eaton, Joshua D., and Steven West. 2020. “Termination of Transcription by RNA Polymerase II: BOOM!” *Trends in Genetics: TIG* 36 (9): 664–75.

1267 Eshed, Yuval, and Zachary B. Lippman. 2019. “Revolutions in Agriculture Chart a Course for
1268 Targeted Breeding of Old and New Crops.” *Science* 366 (6466).
1269 https://doi.org/10.1126/science.aax0025.
1270 F de Felippes, Felipe, Marcus McHale, Rachel L. Doran, Sally Roden, Andrew L. Eamens, E.
1271 Jean Finnegan, and Peter M. Waterhouse. 2020. “The Key Role of Terminators on the
1272 Expression and Post-Transcriptional Gene Silencing of Transgenes.” *The Plant Journal:*
1273 *For Cell and Molecular Biology* 104 (1): 96–112.
1274 Felippes, Felipe F. de, and Peter M. Waterhouse. 2023. “Plant Terminators: The Unsung
1275 Heroes of Gene Expression.” *Journal of Experimental Botany* 74 (7): 2239–50.
1276 Felippes, Felipe Fenselau de, Kylie Shand, and Peter M. Waterhouse. 2022. “Identification of a
1277 Transferrable Terminator Element That Inhibits Small RNA Production and Improves
1278 Transgene Expression Levels.” *Frontiers in Plant Science* 13 (May): 877793.
1279 Griesemer, Dustin, James R. Xue, Steven K. Reilly, Jacob C. Ulirsch, Kalki Kukreja, Joe R.
1280 Davis, Masahiro Kanai, et al. 2021. “Genome-Wide Functional Screen of 3’UTR Variants
1281 Uncovers Causal Variants for Human Disease and Evolution.” *Cell* 184 (20): 5247–60.e19.
1282 Hickey, Lee T., Amber N Hafeez, Hannah Robinson, Scott A. Jackson, Soraya C. M. Leal-
1283 Bertioli, Mark Tester, Caixia Gao, Ian D. Godwin, Ben J. Hayes, and Brande B. H. Wulff.
1284 2019. “Breeding Crops to Feed 10 Billion.” *Nature Biotechnology* 37 (7): 744–54.
1285 Hirai, Tadayoshi, Natsuko Kurokawa, Narendra Duhita, Kyoko Hiwasa-Tanase, Kazuhisa Kato,
1286 Ko Kato, and Hiroshi Ezura. 2011. “The HSP Terminator of Arabidopsis Thaliana Induces a
1287 High Level of Miraculin Accumulation in Transgenic Tomatoes.” *Journal of Agricultural and*
1288 *Food Chemistry* 59 (18): 9942–49.
1289 Huang, Gao, Zhuang Liu, Laurens Van Der Maaten, and Kilian Q. Weinberger. 2017. “Densely
1290 Connected Convolutional Networks.” In *2017 IEEE Conference on Computer Vision and*
1291 *Pattern Recognition (CVPR)*. IEEE. https://doi.org/10.1109/cvpr.2017.243.
1292 Hunt, A. G. 1994. “Messenger RNA3’end Formation in Plants.” *Annual Review of Plant Biology*.
1293 Hunt, Arthur G. 2011. “RNA Regulatory Elements and Polyadenylation in Plants.” *Frontiers in*
1294 *Plant Science* 2: 109.
1295 ———. 2022. “Review: Mechanisms Underlying Alternative Polyadenylation in Plants - Looking
1296 in the Right Places.” *Plant Science: An International Journal of Experimental Plant Biology*
1297 324 (November): 111430.
1298 Hunt, Arthur G., Denghui Xing, and Qingshun Q. Li. 2012. “Plant Polyadenylation Factors:
1299 Conservation and Variety in the Polyadenylation Complex in Plants.” *BMC Genomics* 13
1300 (November): 641.
1301 Ingelbrecht, I. L., L. M. Herman, R. A. Dekeyser, M. C. Van Montagu, and A. G. Depicker. 1989.
1302 “Different 3’ End Regions Strongly Influence the Level of Gene Expression in Plant Cells.”
1303 *The Plant Cell* 1 (7): 671–80.
1304 Jafar, Zehra, Salma Tariq, Irfan Sadiq, Tayyab Nawaz, and Malik Nadeem Akhtar. 2019.
1305 “Genome-Wide Profiling of Polyadenylation Events in Maize Using High-Throughput
1306 Transcriptomic Sequences.” *G3* 9 (8): 2749–60.
1307 Jores, T., M. Hamm, J. T. Cuperus, and C. Queitsch. 2023. “Frontiers and Techniques in Plant
1308 Gene Regulation.” *Current Opinion in Plant Biology* , (in press).
1309 Jores, Tobias, Jackson Tonnies, Michael W. Dorrity, Josh T. Cuperus, Stanley Fields, and
1310 Christine Queitsch. 2020. “Identification of Plant Enhancers and Their Constituent Elements
1311 by STARR-Seq in Tobacco Leaves.” *The Plant Cell* 32 (7): 2120–31.
1312 Jores, Tobias, Jackson Tonnies, Travis Wrightsman, Edward S. Buckler, Josh T. Cuperus,
1313 Stanley Fields, and Christine Queitsch. 2021. “Synthetic Promoter Designs Enabled by a
1314 Comprehensive Analysis of Plant Core Promoters.” *Nature Plants* 7 (6): 842–55.
1315 Kechin, Andrey, Uljana Boyarskikh, Alexander Kel, and Maxim Filipenko. 2017. “cutPrimers: A
1316 New Tool for Accurate Cutting of Primers from Reads of Targeted Next Generation
1317 Sequencing.” *Journal of Computational Biology: A Journal of Computational Molecular Cell*

Biology 24 (11): 1138–43.
Keith, Brian, and Nam-Hai Chua. 1986. “Monocot and Dicot Pre-mRNAs Are Processed with Different Efficiencies in Transgenic Tobacco.” *The EMBO Journal*.
Kertesz, S., Z. Kerenyi, Z. Merai, and I. Bartos. 2006. “Both Introns and Long 3′-UTRs Operate as Cis-Acting Elements to Trigger Nonsense-Mediated Decay in Plants.” *Nucleic Acids*.
Klie, Adam, Hayden Stites, Tobias Jores, Joe J. Solvason, Emma K. Farley, and Hannah Carter. 2022. “EUGENe: A Python Toolkit for Predictive Analyses of Regulatory Sequences.” *bioRxiv*. https://doi.org/10.1101/2022.10.24.513593.
Krzyszton, Michal, Monika Zakrzewska-Placzek, Aleksandra Kwasnik, Norbert Dojer, Wojciech Karlowski, and Joanna Kufel. 2018. “Defective XRN3-Mediated Transcription Termination in Arabidopsis Affects the Expression of Protein-Coding Genes.” *The Plant Journal: For Cell and Molecular Biology* 93 (6): 1017–31.
Kumar, Ananthanarayanan, Marcello Clerici, Lena M. Muckenfuss, Lori A. Passmore, and Martin Jinek. 2019. “Mechanistic Insights into mRNA 3’-End Processing.” *Current Opinion in Structural Biology* 59 (December): 143–50.
Langmead, Ben, and Steven L. Salzberg. 2012. “Fast Gapped-Read Alignment with Bowtie 2.” *Nature Methods* 9 (4): 357–59.
Li, Heng, Bob Handsaker, Alec Wysoker, Tim Fennell, Jue Ruan, Nils Homer, Gabor Marth, Goncalo Abecasis, Richard Durbin, and 1000 Genome Project Data Processing Subgroup. 2009. “The Sequence Alignment/Map Format and SAMtools.” *Bioinformatics* 25 (16): 2078–79.
Liu, Min, Jiafu Zhu, and Zhicheng Dong. 2021. “Immediate Transcriptional Responses of Arabidopsis Leaves to Heat Shock.” *Journal of Integrative Plant Biology* 63 (3): 468–83.
Loke, Johnny C., Eric A. Stahlberg, David G. Strenski, Brian J. Haas, Paul Chris Wood, and Qingshun Quinn Li. 2005. “Compilation of mRNA Polyadenylation Signals in Arabidopsis Revealed a New Signal Element and Potential Secondary Structures.” *Plant Physiology* 138 (3): 1457–68.
Luehrsen, K. R., and V. Walbot. 1994. “Intron Creation and Polyadenylation in Maize Are Directed by AU-Rich RNA.” *Genes & Development* 8 (9): 1117–30.
Luo, Weifei, Arlen W. Johnson, and David L. Bentley. 2006. “The Role of Rat1 in Coupling mRNA 3’-End Processing to Transcription Termination: Implications for a Unified Allosteric-Torpedo Model.” *Genes & Development* 20 (8): 954–65.
Masella, Andre P., Andrea K. Bartram, Jakub M. Truszkowski, Daniel G. Brown, and Josh D. Neufeld. 2012. “PANDAseq: Paired-End Assembler for Illumina Sequences.” *BMC Bioinformatics* 13 (February): 31.
Mogen, B. D., M. H. MacDonald, R. Graybosch, and A. G. Hunt. 1990. “Upstream Sequences Other than AAUAAA Are Required for Efficient Messenger RNA 3’-End Formation in Plants.” *The Plant Cell* 2 (12): 1261–72.
Mogen, B. D., M. H. MacDonald, G. Leggewie, and A. G. Hunt. 1992. “Several Distinct Types of Sequence Elements Are Required for Efficient mRNA 3’ End Formation in a Pea rbcS Gene.” *Molecular and Cellular Biology* 12 (12): 5406–14.
Mo, Weipeng, Bo Liu, Hong Zhang, Xianhao Jin, Dongdong Lu, Yiming Yu, Yuelin Liu, et al. 2021. “Landscape of Transcription Termination in Arabidopsis Revealed by Single-Molecule Nascent RNA Sequencing.” *Genome Biology* 22 (1): 322.
Nagaya, Shingo, Kazue Kawamura, Atsuhiko Shinmyo, and Ko Kato. 2010. “The HSP Terminator of Arabidopsis Thaliana Increases Gene Expression in Plant Cells.” *Plant & Cell Physiology* 51 (2): 328–32.
Nagy, F., G. Morelli, R. T. Fraley, S. G. Rogers, and N. H. Chua. 1985. “Photoregulated Expression of a Pea rbcS Gene in Leaves of Transgenic Plants.” *The EMBO Journal* 4 (12): 3063–68.
Paszke, Adam, Sam Gross, Francisco Massa, Adam Lerer, James Bradbury, Gregory Chanan,

Trevor Killeen, et al. 2019. “Pytorch: An Imperative Style, High-Performance Deep Learning Library.” *Advances in Neural Information Processing Systems* 32.

Pérez-González, Ana, and Elena Caro. 2018. “Effect of Transcription Terminator Usage on the Establishment of Transgene Transcriptional Gene Silencing.” *BMC Research Notes* 11 (1): 511.

Proudfoot, Nick J. 2011. “Ending the Message: poly(A) Signals Then and Now.” *Genes & Development* 25 (17): 1770–82.

Qin, Cheng, Nongnong Shi, Mei Gu, Hang Zhang, Bin Li, Jiajia Shen, Atef Mohammed, et al. 2012. “Involvement of RDR6 in Short-Range Intercellular RNA Silencing in Nicotiana Benthamiana.” *Scientific Reports* 2 (June): 467.

Rodríguez-Leal, Daniel, Zachary H. Lemmon, Jarrett Man, Madelaine E. Bartlett, and Zachary B. Lippman. 2017. “Engineering Quantitative Trait Variation for Crop Improvement by Genome Editing.” *Cell* 171 (2): 470–80.e8.

Rosonina, Emanuel, Syuzo Kaneko, and James L. Manley. 2006. “Terminating the Transcript: Breaking up Is Hard to Do.” *Genes & Development* 20 (9): 1050–56.

Rothnie, H. M. 1996. “Plant mRNA 3’-End Formation.” *Plant Molecular Biology* 32 (1-2): 43–61.

Rothnie, H. M., J. Reid, and T. Hohn. 1994. “The Contribution of AAUAAA and the Upstream Element UUUGUA to the Efficiency of mRNA 3′-End Formation in Plants.” *The EMBO Journal* 13 (9): 2200–2210.

Sanfaçon, H., P. Brodmann, and T. Hohn. 1991. “A Dissection of the Cauliflower Mosaic Virus Polyadenylation Signal.” *Genes & Development* 5 (1): 141–49.

Shen, Yingjia, Guoli Ji, Brian J. Haas, Xiaohui Wu, Jianti Zheng, Greg J. Reese, and Qingshun Quinn Li. 2008. “Genome Level Analysis of Rice mRNA 3′-End Processing Signals and Alternative Polyadenylation.” *Nucleic Acids Research* 36 (9): 3150–61.

Shrikumar, Avanti, Peyton Greenside, and Anshul Kundaje. 2017. “Learning Important Features Through Propagating Activation Differences.” In *International Conference on Machine Learning*, 3145–53. PMLR.

Shrikumar, Avanti, Katherine Tian, Žiga Avsec, Anna Shcherbina, Abhimanyu Banerjee, Mahfuza Sharmin, Surag Nair, and Anshul Kundaje. 2018. “Technical Note on Transcription Factor Motif Discovery from Importance Scores (TF-MoDISco) Version 0.5.6.5.” *arXiv [cs.LG]*. arXiv. http://arxiv.org/abs/1811.00416.

Singh, Ratnesh, Ray Ming, and Qingyi Yu. 2016. “Comparative Analysis of GC Content Variations in Plant Genomes.” *Tropical Plant Biology* 9 (3): 136–49.

Smith, Tom, Andreas Heger, and Ian Sudbery. 2017. “UMI-Tools: Modeling Sequencing Errors in Unique Molecular Identifiers to Improve Quantification Accuracy.” *Genome Research* 27 (3): 491–99.

Sullivan, Alessandra M., Andrej A. Arsovski, Janne Lempe, Kerry L. Bubb, Matthew T. Weirauch, Peter J. Sabo, Richard Sandstrom, et al. 2014. “Mapping and Dynamics of Regulatory DNA and Transcription Factor Networks in A. Thaliana.” *Cell Reports* 8 (6): 2015–30.

Szabo, Emese Xochitl, Philipp Reichert, Marie-Kristin Lehniger, Marilena Ohmer, Marcella de Francisco Amorim, Udo Gowik, Christian Schmitz-Linneweber, and Sascha Laubinger. 2020. “Metabolic Labeling of RNAs Uncovers Hidden Features and Dynamics of the Arabidopsis Transcriptome.” *The Plant Cell* 32 (4): 871–87.

Takagaki, Y., and J. L. Manley. 1997. “RNA Recognition by the Human Polyadenylation Factor CstF.” *Molecular and Cellular Biology* 17 (7): 3907–14.

Thomas, Patrick E., Xiaohui Wu, Man Liu, Bobby Gaffney, Guoli Ji, Qingshun Q. Li, and Arthur G. Hunt. 2012. “Genome-Wide Control of Polyadenylation Site Choice by CPSF30 in Arabidopsis.” *The Plant Cell* 24 (11): 4376–88.

Tian, Bin, and Joel H. Graber. 2012. “Signals for Pre-mRNA Cleavage and Polyadenylation.” *Wiley Interdisciplinary Reviews. RNA* 3 (3): 385–96.

1420 Tian, Chenfei, Yixin Zhang, Jianhua Li, and Yong Wang. 2022. “Benchmarking Intrinsic
1421 Promoters and Terminators for Plant Synthetic Biology Research.” *BioDesign Research*
1422 2022. https://downloads.spj.sciencemag.org/bdr/2022/9834989.pdf.
1423 Tonnies, Jackson, Mueth Nicholas Arthur, Sayeh Gorjifard, Jonah Chu, and Christine Queitsch.
1424 2023. “Scalable Transfection of Maize Mesophyll Protoplasts.” *Journal of Visualized*
1425 *Experiments*, (in press).
1426 Wang, Po-Hao, Sandeep Kumar, Jia Zeng, Robert McEwan, Terry R. Wright, and Manju Gupta.
1427 2020. “Transcription Terminator-Mediated Enhancement in Transgene Expression in Maize:
1428 Preponderance of the AUGAAU Motif Overlapping With Poly(A) Signals.” *Frontiers in Plant*
1429 *Science* 11. https://doi.org/10.3389/fpls.2020.570778.
1430 Wang, Xingang, Lyndsey Aguirre, Daniel Rodríguez-Leal, Anat Hendelman, Matthias Benoit,
1431 and Zachary B. Lippman. 2021. “Dissecting Cis-Regulatory Control of Quantitative Trait
1432 Variation in a Plant Stem Cell Circuit.” *Nature Plants* 7 (4): 419–27.
1433 Washburn, Jacob D., Maria Katherine Mejia-Guerra, Guillaume Ramstein, Karl A. Kremling,
1434 Ravi Valluru, Edward S. Buckler, and Hai Wang. 2019. “Evolutionarily Informed Deep
1435 Learning Methods for Predicting Relative Transcript Abundance from DNA Sequence.”
1436 *Proceedings of the National Academy of Sciences of the United States of America* 116
1437 (12): 5542–49.
1438 Whitelaw, E., and N. Proudfoot. 1986. “Alpha-Thalassaemia Caused by a poly(A) Site Mutation
1439 Reveals That Transcriptional Termination Is Linked to 3’ End Processing in the Human
1440 Alpha 2 Globin Gene.” *The EMBO Journal* 5 (11): 2915–22.
1441 Wu, Xiaohui, Man Liu, Bruce Downie, Chun Liang, Guoli Ji, Qingshun Q. Li, and Arthur G. Hunt.
1442 2011. “Genome-Wide Landscape of Polyadenylation in Arabidopsis Provides Evidence for
1443 Extensive Alternative Polyadenylation.” *Proceedings of the National Academy of Sciences*
1444 *of the United States of America* 108 (30): 12533–38.
1445 Yao, Youli, Luhua Song, Yael Katz, and Gad Galili. 2002. “Cloning and Characterization of
1446 Arabidopsis Homologues of the Animal CstF Complex That Regulates 3’ mRNA Cleavage
1447 and Polyadenylation.” *Journal of Experimental Botany* 53 (378): 2277–78.
1448 Ye, Congting, Qian Zhou, Xiaohui Wu, Guoli Ji, and Qingshun Quinn Li. 2019. “Genome-Wide
1449 Alternative Polyadenylation Dynamics in Response to Biotic and Abiotic Stresses in Rice.”
1450 *Ecotoxicology and Environmental Safety* 183 (November): 109485.
1451 Yu, Xuhong, Pascal G. P. Martin, and Scott D. Michaels. 2019. “BORDER Proteins Protect
1452 Expression of Neighboring Genes by Promoting 3’ Pol II Pausing in Plants.” *Nature*
1453 *Communications* 10 (1): 4359.
1454 Zhang, Jian, Yi-Zhe Zhang, Jing Jiang, and Cheng-Guo Duan. 2020. “The Crosstalk Between
1455 Epigenetic Mechanisms and Alternative RNA Processing Regulation.” *Frontiers in Genetics*
1456 11 (August): 998.
1457 Zhou, Andy, Liam D. Kirkpatrick, Izaiah J. Ornelas, Lorenzo J. Washington, Niklas F. C.
1458 Hummel, Christopher W. Gee, Sophia N. Tang, Collin R. Barnum, Henrik V. Scheller, and
1459 Patrick M. Shih. 2023. “A Suite of Constitutive Promoters for Tuning Gene Expression in
1460 Plants.” *ACS Synthetic Biology* 12 (5): 1533–45.
1461 Zrimec, Jan, Christoph S. Börlin, Filip Buric, Azam Sheikh Muhammad, Rhongzen Chen,
1462 Verena Siewers, Vilhelm Verendel, Jens Nielsen, Mats Töpel, and Aleksej Zelezniak. 2020.
1463 “Deep Learning Suggests That Gene Expression Is Encoded in All Parts of a Co-Evolving
1464 Interacting Gene Regulatory Structure.” *Nature Communications* 11 (1): 6141.